Entanglement Harvesting and Divergences in Unruh-DeWitt Detector Pairs

by

Allison Sachs

A thesis

presented to the University Of Waterloo

in fulfilment of the

thesis requirement for the degree of

Master of Science

in

Physics (Quantum Information)

Waterloo, Ontario, Canada, 2017

I hereby declare that I am the sole author of this thesis. This is a true copy of the thesis, including any required final revisions, as accepted by my examiners.

I understand that my thesis may be made electronically available to the public.

Abstract

We analyze correlations between pairs of detectors quadratically coupled to real and complex scalar bosonic fields in 3+1 dimensions. This is a first step toward studying the entanglement structure of the fermionic vacuum through the entanglement harvesting protocol. We find that, while a single quadratically coupled Unruh-DeWitt presents no divergences, when one considers pairs of detectors there emerge persistent divergences (not regularizable via smooth switching or smearing) in the entanglement they acquire from the field. These divergences were not anticipated in previous studies. We characterize the divergences, discuss whether a suitable regularization can allow for fair comparison of the entanglement harvesting ability of the quadratic and the linear couplings, and finally find a UV-safe quantifier of harvested correlations.

One paper, submitted for publication, comprises the majority of work done in this thesis [1]

Acknowledgements

First I would like to thank my supervisors, Robert B. Mann and Edudardo Martín-Martínez. Robb and Edu, without you I wouldn't be here, and here is exactly where I want to be. Thank you for your mentorship, kindness, and discussions of all sorts (religion, equity, science, philosophy...). Thank you also, of course, for the money to live, conference funding, and other material support. Edu, your overwhelming support, mentorship, and honest, critical feedback continues to be among the most valuable aspects of my graduate degree.

This work was financially supported in part by the Natural Sciences and Engineering Research Council of Canada. Additional financial support was provided by the Department of Physics and Astronomy at the university of Waterloo. Travel grants were provided by the Graduate Studies office at the University of Waterloo, Yukawa Institute for Theoretical Physics, and the University of Queensland. Technical support from friendly and approachable people was provided by the Institute for Quantum Computing at the University of Waterloo. Thank you, QuTask!

In no particular order:

Thank you Emma McKay for your friendship, discussions and support throughout my masters project, and beyond that, for pushing me to be kinder everyday.

Thank you Paulina Corona-Ugalde, Lauren Byl, Judy McDonnell for indispensable aid during the writing of my thesis.

Thank you to my peers in research, Emma McKay, Nayeli Rodriges-Briones, Paulina Corona-Ugalde, Alejandro Pozas Kerstjens, José de Ramon, Nicholas Funai, Laura Henderson, Dan Grimmer, Richard Lopp, Maria Papageorgiou, and so many others for helpful discussions.

Thank you Robie Hennegar for being a swell dude.

Thank you FemPhys for all the work y'all have done and continue to do in community building, all of which has been indispensable to my mental well being during my masters project.

Thank you to all the badass bosses I've encountered in my life, in whose existence I see my own hopes manifest. These folk include (but are certainly not limited to) Cohl Furey,

Christine Nattrass, Caroline Bowen, Cary Earnest, Melanie Campbell, and the professor who stood up at a conference (that I was at as a second year in undergrad) to inform a speaker that the women the speaker was addressing were, in fact, women and not 'girls.' That was a singular moment for me. And of course, unquestionably belonging in this group of steel-strong folk are my mother, aunts, Annette, Nanny, Mee-Maw, Grand 'B' and Granny Belle, although not all of you are still here, you all shape how I walk through this world.

Thank you Kiley Rider for your kindness and helpfulness above and beyond during my application/acceptance to Waterloo. I'll never forget how much your reassurance meant to me, although I don't know if you ever knew.

Thank you Heather Anderson for being *the* admin/staff person in the department who knows whats up, who brightens folk's day, and who is doing the work it takes to bring the physics department closer to being the community its members deserve.

Thank you Jodi, Kim, Marin, Erika, Chris, Sara and the rest of the IQC staff for the hard and valuable work y'all do to make the IQC into a community and not just an institute.

Thank you to all of my parents, Mom, Dad and Ron, for y'all's advice, emotional support, financial support, and for a place to come back to in my worldly travels. Ron: ***Ga-Gaaaaaa***. Dad, thank you for trying to explain integrals to me in Cracker Barrel when I was young, and for trying to explain relativity to me as well (you've got Galilean relativity with trains and tenis balls down pat). Mom, I don't know how to say what I want to say to you with out saying you're the best mom ever. Because you are. Thank you for being an incredible person, and on top of that, the best Mama-Llama in all of existence.

Thank you to all my friends who I haven't thanked yet. Y'all deserve more appreciation than can fit in the Library of Babel (and to at least one of you I owe a book from it), Lindsay, Will, Cary, Morgan, Julia, Abel, Nayeli, John, Joel, Romain, Setphanie, Simon, Cliff, and so many more.

Thank you, GSA-UW folk, for trying to make a difference for graduate students at UW and for letting me work along side you, especially you, Rose and Norman. And thank you PhyGSA folk, especially Jen, for trying to reignite something dearly needed in the physics department.

Thank *you* for reading this thesis! I am so sorry if I've not put your name above and you feel deserving of thanks. You so likely are. You are among an incredible number of people in my life who are deserving of far more than I've stated above. Thank you. I am so lucky to know you all.

Dedication

JAX: I would rather build mud towns by the pond and discover broken, antique forest-junk with you than do any other conceivable thing. Please don't ever stop building and discovering.

Contents

Figures

Abbreviations

eg.	*exempli gratia* for the sake of example.
i.e.	*id est* that is.
LMI	light-matter interaction.
LOCC	local operations and classical communication.
QFT	quantum field theory.
RQI	relativistic quantum information.
UDW	Unruh-DeWitt.
UV	ultra-violet.
VEP	vacuum excitation probability.
wrt	with respect to.

List of Symbols

$*$	Convolution product (defined on page 15).
$:$	Normal ordering.
α	Dimensionless parameter quantifying energy gap in terms of the scale set by the switching time, $\alpha = \Omega T$.
β	Dimensionless parameter quantifying detector separation in terms of the scale set by the switching time, $\beta = \lvert\boldsymbol{x}...\rvert/T$.
Chi	Cosine hyperbolic integral function (defined on page 28).
χ	Switching function. Controls the time-dependence of the coupling strength.
δ	Dimensionless parameter quantifying a detector's spatial extent in terms of the scale set by the switching time, $\delta = \sigma/T$.
Ei	Exponential integral (defined on page 19).
ϵ	UV cutoff.
erf	Error function (defined on page 16).
erfc	Complementary error function (defined on page 17).
erfi	Imaginary error function (defined on page 16).
η	Dimensionless parameter quantifying UV cutoff in terms of the scale set by the switching time, $\eta = \epsilon T$.
F	Spatial profile. Controls the shape and size of the detector.
$\mathcal{F}$	Fourier transform (defined on page 15).
γ	Dimensionless parameter quantifying a detector's switch-on-time in terms of the scale set by the switching time, $\gamma_\nu = t_\nu T$.
$\hat{H}$	Hamiltonian. In this work, generally the Hamiltonian of a particular UDW detector model.
I	Mutual information (defined on page 6).

$\mathcal{L}$ Density matrix elements which, at leading order, contribute to the strength of total correlations ($\mathcal{L}_{\text{AB}}$) or local noise in the system ($\mathcal{L}_{\text{AA}}$).

$\mathcal{L}_0$ Lagrangian.

λ Coupling constant. Controls the overall strength of the interaction.

$\mathcal{M}$ Density matrix element which, at leading order, contributes to the strength of the entanglement negativity.

$\hat{\mu}$ Monopole moment. Describes the two-level internal degree of freedom of the detector (defined on page 7).

$\mathcal{N}$ Entanglement negativity (defined on page 5).

Ω Energy gap.

$\hat{\phi}$ Field operator.

$^{\hat{\Phi}\hat{\Phi}^\dagger}$ This superscript indicates association with the quadratic, complex-field detector model.

$^{\hat{\phi}^2}$ This superscript indicates association with the quadratic, real-field detector model.

$^{\hat{\phi}}$ This superscript indicates association with the linear detector model.

Shi Sine hyperbolic integral function (defined on page 28).

σ Size of detector, OR...

σ ...The set of eigenvalues (spectrum) of a matrix.

sinh Hyperbolic sine function.

t_ν Time of peak coupling (center of switching function) of detector ν.

Tr Trace. If there is a subscript, then it denotes the partial trace with respect to (wrt) some subsystem.

W Wightman function. In the case of the linear detector, it is the same as the two-point correlation function.

$\boldsymbol{x}_\nu$ Position of detector ν.

ξ Dimensionless variable of integration without a physical interpretation, defined in terms of the scale set by the switching time, $\xi = q/T$.

Quote

,,Oooh! Ya wicked Ay! Wicked Ay! Oooh hooh! Say No MORE!."

-Eric Idle

Chapter 1

Introduction

Motivation: Fermionic entanglement ambiguities

Is there an unambiguous way to characterize the entanglement of the fermionic field between two disjoint regions of spacetime?

The answer to this question is not uncontroversial [2–19]. Due to the anti-commuting properties and parity conservation of fermions, notions of separability and entanglement that are all equivalent for bosons are in fact different for fermonic systems [20]. Fermionic Entanglement is also affected by superselection rules [21–25]. Additionally, as has been pointed out in the literature, in the past many studies of the entanglement structure of fermionic systems have not fully taken into account the subtleties associated with the braiding statistics of fermionic fields [5, 6, 10, 26–32].

One way to avoid these subtle issues with fermionic entanglement structure is to probe fermionic systems with localized detectors (see Section 2.4). The detectors can become entangled or not depending on the entanglement present in the field. The study of entanglement through particle detectors in the bosonic case has become known as entanglement harvesting [33–36]. This protocol will allow us to operationally characterize fermionic entanglement structure and make a comparison to the bosonic field.

A model describing a detector coupling to a fermionic field has existed in the literature for quite some time [37–39]. However, previous studies focused only on transition rates, and suffered divergences that needed careful treatment. Additionally, it was pointed out that the models of fermionic particle detectors were riddled with persistent divergences that made it impossible to compute anything but transition rates. For the study of entanglement harvesting we need to fully characterize the detector's density matrix [40]. Additionally, in order to apply this detector model to the entanglement harvesting scenario, one must use pairs of detectors. The renormalization study only considered the single detector and thus could not consider the entanglement structure of the field. This motivates the future study of pairs of detectors coupling to fermionic fields.

However, the fermionic detector model described above necessarily utilizes a quadratic coupling to the field, as we will discuss more in depth later [40]. Because the coupling of the fermionic detector model is quadratic and therefore necessarily different from the coupling in the bosonic detector model primarily considered in the literature, we need to characterize the quadratic bosonic detector model in addition to the fermionic model. This will give us clues as to the source of any differences that may arise between the fermionic and bosonic detector models. The differences could come from analytic structure (spinor versus scalar), spin-statistics (fermionic versus bosonic) or the coupling (linear versus quadratic). Only then can we make an equal-footing comparison of bosonic and fermionic entanglement.

Thus we arrive at the goal of this thesis: to understand how the quadratic coupling changes the character of the bosonic detector.

Context: Relativistic quantum information

This thesis is a contribution to the field of relativistic quantum information (RQI), which, for the purposes of this work, we we will define as the study of the intersection of three major fields: quantum theory, relativity, and information theory.

Early results in RQI studied entanglement in various settings, primarily between field modes in curved spacetimes or accelerated frames. These studies often relied on Bogoliubov transformations and the single mode approximation. Being limited by issues of localization and identification of observable quantities [10,11,41], an alternative to this bumpy road is to work with Unruh-DeWitt (UDW) detectors, which provide localized and physically interpretable results. Additionally, with the UDW detector came a notion of particle as "that which a particle detector detects" [42].

Detectors in quantum fields are only a small aspect of work being done in RQI, although particle detector approaches to field theory are the most relevant work to this thesis. Another research direction includes experimental proposals probing general relativistic effects in quantum scenarios, such as time dilation of clocks and interference of photons [43–45]. Additionally there are more foundational questions being asked, such as those related to causal structure of spacetime [46,47], the connection between information and energy flows in quantum fields [48–50], black holes and information loss [6,6,11,51–55] or the study of causality issues in quantum systems [56]. RQI is also concerned with the light-matter interaction and how simplifications may break down when under the scrutiny of relativistic concerns (see, among many others, [50, 57–61]).

Results: Divergences and entanglement harvesting

This thesis will present, along with the relevant context, an analysis of pairs of detectors quadratically coupled to scalar bosonic fields. We then we show the relationship between the complex bosonic detector model and the real quadratic detector model.

We will find that the quadratic model for pairs of detectors presents a divergence. This divergence shows up at leading order in perturbation theory despite the choice of smooth detector shapes and application of the renormalization scheme that successfully renormalized the single quadratic model.

To regularize this divergence we will introduce a UV cutoff. For a given UV cutoff, we find that the quadratic detector model exhibits qualitatively similar mutual information and entanglement harvesting capabilities. However, the UV cutoff dictates which model harvests more entanglement.

Finding that the quadratic model exhibited divergences, we looked for UV safe quantifiers of correlations. We found the mutual information to be convergent in the limit of removing the UV cutoff.

Chapter 2

Review

2.1 Entanglement harvesting

The vacuum state of a quantum field displays quantum correlations between observables defined in spacelike separated regions [62, 63]. This vacuum entanglement has been studied in quantum foundations, and has found a variety of applications such as quantum energy teleportation [49, 64], the black hole information loss problem [65] and firewalls, along with black hole complementarity [53, 54].

In a phenomenon called *entanglement harvesting* [66], correlations in a quantum field (such as the electromagnetic field) can be swapped to particle detectors (such as atoms or qubits, see Section 2.4). This is possible even when the particle detectors remain spacelike separated throughout the duration of their interaction with the field. This was first shown by Valentini [33] and later by Reznik et al. [34, 35].

Since then, entanglement harvesting has been shown to be sensitive to the background geometry of spacetime [67–69], as well as the topology [70]. Additionally, it has been shown that entanglement harvesting can be done sustainably and distilled into Bell pairs in a process called *entanglement farming* [71]. This kind of process has also found applications within quantum metrology, for example in the detection of vibration (quantum seismometer) [72] or range-finding [66]. Entanglement harvesting has also been studied in detail in timelike separation contexts [73, 74] with implementation proposals in different testbeds from quantum key distribution based on homodyne detection [75] to strongly coupled superconducting qubits [76].

To model the entanglement-swapping interaction between the detectors and field, the Unruh-DeWitt detector model is used (see Section 2.4). For the entanglement harvesting protocol, this model utilizes a pair of first-quantized system (called a detector) linearly coupled to a scalar bosonic field. While most of our knowledge of entanglement harvesting has been gleaned from this setup [58, 67–72], there has been some exploration of more realistic models such as electromagnetic coupling of atoms [77]. All these studies,

however, analyzed entanglement harvesting for bosonic fields.

It is known from fundamental studies that there are differences between the entanglement structure of the vacuum of fermionic and bosonic fields [2–19]. However, a study of entanglement harvesting in fermionic setups has never been performed. A study of detector-based entanglement harvesting from a fermionic vacuum could resolve ambiguities in defining entanglement measures between disjoint regions of a fermionic field [2–4, 14–19]. The reasons why this has not been done can be traced back to fundamental difficulties associated with particle detector models for fermionic fields, and the need for a renormalization scheme, as originally outlined in [40].

2.2 Some aspects of correlations in quantum theory

There are many different ways of quantifying correlations, depending on the type of correlation of interest (eg. total correlations, entanglement) and the type of state(s) under consideration (eg. mixed or pure, bi- or multi-partite). For the remainder of this thesis we will be concerned with total correlations and entanglement of mixed bipartite quantum states.

Entanglement can be quantified (measured) by any map that is non-increasing under local operations and classical communication (LOCC), such as entanglement of formation [78] and distillable entanglement [79], neither of which is efficiently computable [80]. In this paper we will use entanglement negativity, as it is a computable measure of entanglement for mixed bipartite quantum states [80, 81].

2.2.0.1 Entanglement negativity

Entanglement negativity of a bipartite state ρ is an entanglement monotone (under local transformations) defined as

$$\mathcal{N}(\rho) = \frac{||\rho^{\gamma_A}|| - 1}{2}, \tag{2.1}$$

where ρ^{γ_A} denotes the partial transpose of ρ with respect to subsystem A. An equivalent definition is the sum of the negative eigenvalues of the partial transpose of ρ [80]:

$$\mathcal{N}(\rho) = \sum_{\lambda_i \in \sigma[\rho^{\gamma_A}]} \frac{|\lambda_i| - \lambda_i}{2}, \tag{2.2}$$

2.2.0.2 Mutual information

The Mutual Information mutual information $I(\rho_{\mathrm{AB}})$ between two detectors quantifies the amount of uncertainty about one detector that is eliminated if some information

about the state of the other is revealed [82]. Thus, it constitutes a faithful measure of correlations (regardless of if they are classical or quantum) between bipartite quantum quantum states. [83]

In general, for a composite quantum system consisting of two subsystems A and B, the mutual information given by

$$I(\rho_{\text{AB}}) = S(\rho_{\text{A}}) + S(\rho_{\text{B}}) - S(\rho_{\text{AB}}), \tag{2.3}$$

where $\rho_\nu = \text{Tr}_\mu(\rho_{\nu\mu})$ is the partial trace of $\rho_{\nu\mu}$ with respect to subsystem $\mu \in \{A, B\}$ and S is the von Neumann entropy given by $S(\rho) = -\text{Tr}(\rho \log \rho)$.

2.3 Basics of quantum field theory: Scalar fields

In this thesis we shall consider massless, scalar bosonic fields on 3+1 dimensional Minkovski spacetimes. There will be some short discussion of fermionic fields to motivate the quadratic coupling used throughout this work, but knowledge of fermionic fields beyond anything rudimentary is unnecessary for understanding the material that will be presented herein.

Here we present a short introduction to scalar field theory, starting with the action and equations of motion, discussing field expansions and commutation relations, and culminating in a short calculation of the Wightman function and an application of Wick's theorem.

The following review relies on various sources [41, 84–86]

2.3.1 The massless, scalar bosonic field in flat spacetime

The Lagrangian density for a massless free scalar bosonic field, $\hat{\phi}$, is

$$\mathcal{L}_0 = \frac{1}{2}\partial_\mu\hat{\phi}\partial^\mu\hat{\phi}. \tag{2.4}$$

The Klein-Gordon equation minimizes the associated action of Eq. (2.4):

$$\partial_\mu\partial^\mu\hat{\phi} = 0, \tag{2.5}$$

Any solution to the differential equation (2.5) can be written in terms of a basic solution set of functions, eg. plane waves,

$$u_{\boldsymbol{k}} = e^{-\text{i}(|\boldsymbol{k}|t - \boldsymbol{x}\cdot\boldsymbol{k})} \qquad \text{and} \qquad u^*_{\boldsymbol{k}} = e^{\text{i}(|\boldsymbol{k}|t - \boldsymbol{x}\cdot\boldsymbol{k})}, \tag{2.6}$$

which are orthonormal with respect to the Klein Gordon inner product,

$$(\phi_1, \phi_2)_{KG} = i\int d^3x\ \left[\phi_1^*\,\partial_t\,(\phi_2) - (\partial_t\,{\phi_1}^*)\phi_2\right]. \tag{2.7}$$

This 'inner product' is positive definite only for positive frequency solutions, which satisfy

$$\partial_t u_{\boldsymbol{k}}(\boldsymbol{x},t) = -\mathrm{i}\omega u_{\boldsymbol{k}}(\boldsymbol{x},t). \tag{2.8}$$

Now we can express a classical scalar field as

$$\phi(\boldsymbol{x},t) = \int \mathrm{d}^n\boldsymbol{k}\left(a^*_{\boldsymbol{k}}u^*_{\boldsymbol{k}} + a_{\boldsymbol{k}}u_{\boldsymbol{k}}\right), \tag{2.9}$$

where a and a^* are complex amplitudes, which will depend on dimension (n) and $|\boldsymbol{k}|$.

To quantize the field, we impose the canonical commutation relations on the field and its canonical conjugate momentum $\hat{\pi} = \partial_t\hat{\phi}$, promoting them both to operator status:

$$\left[\hat{\phi}(\boldsymbol{x}),\hat{\pi}(\boldsymbol{y})\right] = \mathrm{i}\delta^n\left(\boldsymbol{x}-\boldsymbol{y}\right) \qquad \left[\hat{\phi}(\boldsymbol{x}),\phi(\boldsymbol{y})\right] = \left[\hat{\pi}(\boldsymbol{x}),\pi(\boldsymbol{y})\right] = 0. \tag{2.10}$$

We then promote each complex amplitude a or a^* to a creation or annihilation operator, $\hat{a}_{\boldsymbol{k}}, \hat{a}^\dagger_{\boldsymbol{k}}$. These operators inherit their commutation relations from the canonical commutation relations

$$\left[\hat{a}_{\boldsymbol{k}},\hat{a}^\dagger_{\boldsymbol{k}}\right] = \delta^n\left(\boldsymbol{k}-\boldsymbol{k}'\right) \qquad \left[\hat{a}_{\boldsymbol{k}},\hat{a}_{\boldsymbol{k}}\right] = \left[\hat{a}^\dagger_{\boldsymbol{k}},\hat{a}^\dagger_{\boldsymbol{k}}\right] = 0. \tag{2.11}$$

Thus we can write the full field operator as

$$\hat{\phi}(\boldsymbol{x},t) = \int \frac{\mathrm{d}^n\boldsymbol{k}}{\sqrt{2(2\pi)^n|\boldsymbol{k}|}}\left(\hat{a}^\dagger_k u^*_{\boldsymbol{k}} + \hat{a}_k u_{\boldsymbol{k}}\right). \tag{2.12}$$

where the normalization $1/\sqrt{2(2\pi)^n|\boldsymbol{k}|}$ follows from the commutation relation of the operators $\hat{a}_{\boldsymbol{k}}$ and $\hat{a}^\dagger_{\boldsymbol{k}}$ together with normalization.

2.4 Particle detectors in flat spacetime

Unlike in first quantized systems, there are no position observables in a quantum field theory (QFT). Thus it is difficult to extract spatiotemporal information from them [87]. Meanwhile, all experiments probe finite patches of spacetime. Furthermore, the definition of a particle in QFT is observer dependent, as quantization procedures for different, non-inertial observers produce incompatible fock spaces [52, 88–91]. Reflecting on these difficulties, UDW detectors were introduced as an operational way to circumvent the difficulties in defining the particle content of a bosonic quantum field and to probe localized patches of spacetime [42, 52].

An UDW detector consists of a two-level quantum emitter (detector) coupled linearly to a scalar quantum field along its worldline. For a single inertial detector (labelled A) in flat spacetime, the UDW interaction Hamiltonian in the interaction picture is given by

$$\hat{H}^{\hat{\phi}}(t) = \lambda_{\mathrm{A}}\chi_{\mathrm{A}}(t-t_{\mathrm{A}})\hat{\mu}_{\mathrm{A}}(t)\int \mathrm{d}^n\boldsymbol{x}F_{\mathrm{A}}(\boldsymbol{x}-\boldsymbol{x}_{\mathrm{A}})\hat{\phi}(\boldsymbol{x},t). \tag{2.13}$$

Here, the monopole moment $\hat{\mu}_{\rm A}(t) = \hat{\sigma}^{+}_{\rm A} e^{{\rm i}\Omega_{\rm A} t} + \hat{\sigma}^{-}_{\rm A} e^{-{\rm i}\Omega_{\rm A} t}$ represents the two-level internal degree of freedom of the detector, which couples linearly to a real massless scalar field $\hat{\phi}(\boldsymbol{x}, t)$. $0 \leq \chi_{\rm A}(t) \leq 1$ is the switching function that controls the time-dependence of the coupling of strength λ_A. The spatial profile $F(\boldsymbol{x})$ carries information about the shape and size of the detector. The case of the point-like detector, commonly considered in the literature, is a particular case of (2.13) where the smearing function is a delta distribution, $F_{\rm A}(\boldsymbol{x}) = \delta(\boldsymbol{x})$.

As a quick aside, it is crucial to note that the hamiltonian (2.13) is not time independent if χ is not a constant function. This means that we should not expect energy conservation. This is important particularly when considering the vacuum excitation probability (VEP) of a detector, that is the probability that a detector in its ground state is excited by the vacuum. Further discussion of the energy flows in the UDW model can be found in [59, 92]

Modifications of the UDW model (2.13) where the detector is coupled quadratically to the field [39] allow one to compare on equal footing the response of bosonic and fermionic detectors (the latter necessarily being quadratic [38]). These models have been recently analyzed in detail in [40]. The interaction Hamiltonian for a UDW detector coupled quadratically to a real scalar field is given by

$$\hat{H}^{\hat{\phi}^2}(t) = \lambda_{\rm A} \chi_{\rm A}(t - t_{\rm A}) \hat{\mu}_{\rm A}(t) \int {\rm d}^n \boldsymbol{x}\, F_{\rm A}(\boldsymbol{x} - \boldsymbol{x}_{\rm A}) : \hat{\phi}^2(\boldsymbol{x}, t) :, \tag{2.14}$$

where $\phi^2(\boldsymbol{x}, t)$ has been normal-ordered as prescribed by the analysis in [40]. If the detector couples to a complex (charged) scalar field, then the Hamiltonian takes the form

$$\hat{H}^{\hat{\Phi}\hat{\Phi}^\dagger}(t) = \lambda_{\rm A} \chi_{\rm A}(t - t_{\rm A}) \hat{\mu}_{\rm A}(t) \int {\rm d}^n \boldsymbol{x}\, F_{\rm A}(\boldsymbol{x} - \boldsymbol{x}_{\rm A}) : \hat{\Phi}\, \hat{\Phi}^\dagger :, \tag{2.15}$$

2.4.0.1 Persistent vs. regularizable divergences

It is convenient at this point to define two different types of ultra-violet (UV) divergences that particle detector models may present. A *regularizable* divergence is one that can be removed by use of a smooth switching function and/or a smooth spatial profile (see, e.g., [93–95]). A *persistent* divergence is one that remains even with smooth switching and smearing functions (such as the divergences renormalized in [40]).

Analysis of the detector response function [93–95] and a number of investigations of entanglement harvesting and quantum communication with (linear) UDW detectors [33–36, 59, 64, 66, 77, 96, 97] indicate that all leading order UV divergences present in the time evolution of linearly coupled UDW detectors are regularizable. While this is not the case for quadratically coupled detectors [37–39, 55], it has been shown that all persistent divergences can also be renormalized for an individual quadratically coupled detector [40]. We will demonstrate below that a straightforward application of the

leading-order prescription in [40] cannot renormalize persistent leading-order divergences in more complex scenarios with several detectors.

To analyze fermionic fields from the perspective of localized particle detectors a detector model was introduced that consisted of a cavity coupled to a fermionic field [55], much like Unruh's original detector was a cavity coupled to a bosonic field [52]. Later, Takagi introduced an UDW-like model for fermionic fields [37, 38], wherein a two level system coupled quadratically to a fermionic field,

$$\hat{H}_{\text{F}} \propto \hat{\mu}\overline{\Psi}\Psi. \tag{2.16}$$

However, this model contained persistent divergences that could not be regularized by an appropriate choice of switching and smearing functions, as it was found in [40]. Thus, these investigations restricted themselves to studying transition rates instead of transition probabilities. To track down the origin of these divergences in Takagi's fermionic detector, Hümer et al. studied three types of quadratically coupled UDW-like detectors [40]. They concluded that these divergences are mainly due to the detector coupling quadratically to the field instead of resulting from the analytic structure (spinor vs. scalar) or statistics (fermionic vs. bosonic) of the fields involved. Persistent divergences in the single-detector vacuum excitation probabilities (VEP) of quadratic UDW detectors were found to be renormalizable by the same techniques used in quantum electrodynamics [40], eg. normal ordering the interaction Hamiltonian.

Chapter 3

Results and discussion

In the first three sections of this chapter, we will outline the calculation of the density matrix elements of the three models studied in this paper: a pair of the (usual) linear UDW detectors, a pair of detectors that quadratically couple to a real scalar field, and a pair of detectors that quadratically couple to a charged scalar field. In the fourth and fifth sections of this chapter, we will discuss divergences in the quadratic model and the results of the entanglement harvesting protocol, respectively.

3.1 Linear Unruh-DeWitt detector

We begin by recapitulating results for the linear UDW model [36]. The method of calculation here presents different pros and cons with respect to the numerical properties of the resultant expressions. First, the terms that do not have a closed form in the literature (namely, the terms responsible for entanglement harvesting) were numerically unstable for small energy gap detectors and therefore this region of parameter space has not been explored previously. With the calculations that follow, we are able to study small gap detectors, but with the caveat that now we make the simplifying assumption that the detectors are switched on simultaneously in their comoving frame. This is not a fully general assumption, but one that is necessary to find closed forms for some of the most challenging integrals in the density matrix elements.

The linear UDW Hamiltonian can be rewritten for the two-detector case as a sum over detectors A and B (i.e. there are no detector-detector interactions)

$$\hat{H}^{\hat{\phi}} = \sum_{\nu\in\{\mathrm{A,B}\}} \lambda_\nu \chi_\nu(t-t_\nu)\hat{\mu}_\nu(t) \int \mathrm{d}^n\boldsymbol{x}\, F_\nu(\boldsymbol{x}-\boldsymbol{x}_\nu)\hat{\phi}(\boldsymbol{x},t). \tag{3.1}$$

If we let the initial state of the field-detector system be $\hat{\rho}_0$, its time evolved state is $\hat{\rho}_{_T} = \hat{U}\hat{\rho}_0\hat{U}^\dagger$, where the subscript T denotes the timescale where the switching function

is non-zero. The time evolution operator $\hat{U}$ is given by the time-ordered exponential

$$\hat{U} = \mathcal{T} \exp\left(\int_{-\infty}^{\infty} \mathrm{d}t \hat{H}^{\hat{\phi}}(t)\right). \tag{3.2}$$

Consequently, we can express the time evolution operator $\hat{U}$ in terms of a Dyson expansion as

$$\hat{U} = \mathbb{1} + \hat{U}^{(1)} + \hat{U}^{(2)} + \mathcal{O}(\lambda_\nu^3), \tag{3.3}$$

where

$$\hat{U}^{(1)} = -\mathrm{i} \int_{-\infty}^{\infty} \mathrm{d}t \, \hat{H}_{\mathrm{I}}(t) \tag{3.4}$$

$$\hat{U}^{(2)} = -\int_{-\infty}^{\infty} \mathrm{d}t \int_{-\infty}^{t} \mathrm{d}t' \, \hat{H}_{\mathrm{I}}(t) \hat{H}_{\mathrm{I}}(t'). \tag{3.5}$$

It follows that $\hat{\rho}_{_T}$ can be expressed in a perturbative expansion,

$$\hat{\rho}_{_T} = \hat{\rho}_0 + \hat{\rho}_{_T}^{(1,0)} + \hat{\rho}_{_T}^{(0,1)} + \hat{\rho}_{_T}^{(1,1)} + \hat{\rho}_{_T}^{(2,0)} + \hat{\rho}_{_T}^{(0,2)} + \mathcal{O}(\lambda_\nu^3), \tag{3.6}$$

where $\hat{\rho}_{_T}^{(i,j)} = \hat{U}^{(i)} \hat{\rho}_0 \hat{U}^{(j)\dagger}$.

After time evolution, the time evolved partial state of the detectors is obtained by tracing out the field degrees of freedom:

$$\hat{\rho}_{\mathrm{AB,T}} = \mathrm{Tr}_{\hat{\phi}} \left(\hat{\rho}_{_T}\right). \tag{3.7}$$

If we take the initial state of the field to be its lowest-energy (vacuum) state,

$$\hat{\rho}_0 = |0\rangle\langle 0| \otimes \hat{\rho}_{\mathrm{AB},0}, \tag{3.8}$$

then the first order term $\hat{\rho}_{_T}^{(1,0)} + \hat{\rho}_{_T}^{(0,1)}$ does not contribute at all to the detectors' dynamics (this is the case for all field states whose one-point function is zero, eg. Fock states, free thermal states and therefore the vacuum state). In fact, for the vacuum state it can be easily proved that $\mathrm{Tr}_{\hat{\phi}} \left(\hat{\rho}_{_T}^{(i,j)}\right) = 0$ when $i + j$ is odd (see e.g., [36]). Thus, we can express the time-evolved density matrix of the subsystem consisting of the two detectors as

$$\hat{\rho}_{\mathrm{AB,T}} = \hat{\rho}_{\mathrm{AB},0} + \lambda_{\mathrm{A}}^2 \hat{\rho}_{\mathrm{A,T}} + \lambda_{\mathrm{B}}^2 \hat{\rho}_{\mathrm{B,T}} + \lambda_{\mathrm{A}} \lambda_{\mathrm{B}} \hat{\rho}_{\mathrm{cor,T}} + \mathcal{O}(\lambda_\nu^4), \tag{3.9}$$

where we have separated the local contributions to time evolution (proportional to λ_{A}^2 and λ_{B}^2 at leading order) from the non-local terms (responsible for the correlations the detectors acquire through the field) proportional to $\lambda_{\mathrm{A}} \lambda_{\mathrm{B}}$. Notice that, from Eq. (3.9), we can quickly recover the case of the evolution of a single detector just by taking one of the coupling strengths to zero (e.g. $\lambda_{\mathrm{B}} = 0$).

Let us now particularize to the case where both detectors start out in the ground state:

$$\hat{\rho}_{\mathrm{AB},0} = |g_{\mathrm{A}}\rangle\langle g_{\mathrm{A}}| \otimes |g_{\mathrm{B}}\rangle\langle g_{\mathrm{B}}|. \tag{3.10}$$

It is convenient to pick the usual [36] 4×4 matrix representation for $\hat{\rho}_{\mathrm{AB,T}}$ in the basis

$$\begin{aligned} |g_{\mathrm{A}} g_{\mathrm{B}}\rangle &= (1,0,0,0)^{\dagger}, & |e_{\mathrm{A}} g_{\mathrm{B}}\rangle &= (0,1,0,0)^{\dagger}, \\ |g_{\mathrm{A}} e_{\mathrm{B}}\rangle &= (0,0,1,0)^{\dagger}, & |e_{\mathrm{A}} e_{\mathrm{B}}\rangle &= (0,0,0,1)^{\dagger}. \end{aligned} \tag{3.11}$$

In this basis, $\hat{\rho}_{\mathrm{AB,T}}$ takes the form

$$\hat{\rho}_{\mathrm{AB,T}} = \begin{pmatrix} 1-\mathcal{L}_{\mathrm{AA}}-\mathcal{L}_{\mathrm{BB}} & 0 & 0 & \mathcal{M}^{*} \\ 0 & \mathcal{L}_{\mathrm{AA}} & \mathcal{L}_{\mathrm{AB}} & 0 \\ 0 & \mathcal{L}_{\mathrm{BA}} & \mathcal{L}_{\mathrm{BB}} & 0 \\ \mathcal{M} & 0 & 0 & 0 \end{pmatrix} + \mathcal{O}(\lambda_{\nu}^{4}), \tag{3.12}$$

as in [36]. The detectors coupled quadratially to either real or complex scalar fields take the same form (see sections 3.2, and 3.3), and $\mathcal{M}$ and $\mathcal{L}_{\mu\nu}$ depend on the the field. Additionally, $\mathcal{M}$ and $\mathcal{L}_{\mu\nu}$ depend on the nature of the coupling (e.g. different switching and smearing functions).

The matrix elements of Eq. (3.12) for the linear coupling have been studied at length in the literature (See, for instance, [36], which sets the notation that we will follow here) and are given by

$$\mathcal{M}^{\hat{\phi}} = -\lambda_{\mathrm{A}}\lambda_{\mathrm{B}} \int_{-\infty}^{\infty}\mathrm{d}t \int_{-\infty}^{t}\mathrm{d}t' \int \mathrm{d}^{n}\boldsymbol{x} \int \mathrm{d}^{n}\boldsymbol{x}'\, M(t,\boldsymbol{x},t',\boldsymbol{x}')\, W^{\hat{\phi}}(t,\boldsymbol{x},t',\boldsymbol{x}') \tag{3.13}$$

$$\mathcal{L}_{\nu\mu}{}^{\hat{\phi}} = \lambda_{\nu}\lambda_{\mu} \int_{-\infty}^{\infty}\mathrm{d}t \int_{-\infty}^{\infty}\mathrm{d}t' \int \mathrm{d}^{n}\boldsymbol{x} \int \mathrm{d}^{n}\boldsymbol{x}'\, L_{\nu}^{*}(t,\boldsymbol{x})\, L_{\mu}(t',\boldsymbol{x}')\, W^{\hat{\phi}}(t,\boldsymbol{x},t',\boldsymbol{x}'), \tag{3.14}$$

where the superscript $\hat{\phi}$ denotes linear coupling to the real scalar field and where, assuming that the switching function χ and the smearing function F are real, L_{ν} and $M(t,\boldsymbol{x},t',\boldsymbol{x}')$ are

$$L_{\nu}(t,\boldsymbol{x}) = \chi_{\nu}(t-t_{\nu})\, F_{\nu}(\boldsymbol{x}-\boldsymbol{x}_{\nu})\, e^{\mathrm{i}\Omega_{\nu}t} \tag{3.15}$$

$$M(t,\boldsymbol{x},t',\boldsymbol{x}') = L_{\mathrm{A}}(t,\boldsymbol{x})L_{\mathrm{B}}(t',\boldsymbol{x}') + L_{\mathrm{A}}(t',\boldsymbol{x}')L_{\mathrm{B}}(t,\boldsymbol{x}), \tag{3.16}$$

and the Wightman function, $W^{\hat{\phi}}$ is given by

$$W^{\hat{\phi}}(t,\boldsymbol{x},t',\boldsymbol{x}') = \langle 0|\, \hat{\phi}(\boldsymbol{x},t)\, \hat{\phi}(\boldsymbol{x}',t')\, |0\rangle\,. \tag{3.17}$$

To find an explicit expression for the Wightman function, we will utilize a plane-wave mode expansion of the field operator with regularization ϵ (see section 3.1.0.1 for a discussion of interpreting ϵ as a soft UV cutoff),

$$\hat{\phi}(\boldsymbol{x},t) = \int \frac{\mathrm{d}^{n}\boldsymbol{k}\, e^{-\epsilon|\boldsymbol{k}|/2}}{\sqrt{2(2\pi)^{n}|\boldsymbol{k}|}} \left(\hat{a}_{k}^{\dagger} e^{\mathrm{i}(|\boldsymbol{k}|t-\boldsymbol{k}\cdot\boldsymbol{x})} + \hat{a}_{k} e^{-\mathrm{i}(|\boldsymbol{k}|t-\boldsymbol{k}\cdot\boldsymbol{x})}\right). \tag{3.18}$$

Here, $\hat{a}^\dagger_{\boldsymbol{k}}$ (and $\hat{a}_{\boldsymbol{k}}$) are creation (and annihilation) operators that satisfy the canonical commutation relations $[\hat{a}_{\boldsymbol{k}_1}, \hat{a}^\dagger_{\boldsymbol{k}_2}] = \delta^{(n)}(\boldsymbol{k}_1 - \boldsymbol{k}_2)$.

This mode expansion allows us to write the Wightman function as

$$W^{\hat{\phi}}(t,\boldsymbol{x},t',\boldsymbol{x}') = \langle 0| \left(\int \frac{\mathrm{d}^n\boldsymbol{k}\, e^{-\epsilon|\boldsymbol{k}|/2}}{\sqrt{2(2\pi)^n|\boldsymbol{k}|}} \left(\hat{a}^\dagger_k e^{\mathrm{i}(|\boldsymbol{k}|t - \boldsymbol{k}\cdot\boldsymbol{x})} + \hat{a}_k e^{-\mathrm{i}(|\boldsymbol{k}|t-\boldsymbol{k}\cdot\boldsymbol{x})} \right) \right. \tag{3.19}$$
$$\left. \times \int \frac{\mathrm{d}^n\boldsymbol{k}'\, e^{-\epsilon|\boldsymbol{k}'|/2}}{\sqrt{2(2\pi)^n|\boldsymbol{k}'|}} \left(\hat{a}^\dagger_{\boldsymbol{k}'} e^{\mathrm{i}(|\boldsymbol{k}'|t' - \boldsymbol{k}'\cdot\boldsymbol{x}')} + \hat{a}_{\boldsymbol{k}'} e^{-\mathrm{i}(|\boldsymbol{k}'|t'-\boldsymbol{k}'\cdot\boldsymbol{x}')} \right) \right) |0\rangle \,.$$

Using that $\langle 0|\, \hat{a}^\dagger_{\boldsymbol{k}} = \hat{a}_{\boldsymbol{k}}\, |0\rangle = 0$ we find

$$W^{\hat{\phi}}(t,\boldsymbol{x},t',\boldsymbol{x}') = \int \frac{\mathrm{d}^n\boldsymbol{k}\, e^{-\epsilon|\boldsymbol{k}|/2}}{\sqrt{2(2\pi)^n|\boldsymbol{k}|}} \int \frac{\mathrm{d}^n\boldsymbol{k}'\, e^{-\epsilon|\boldsymbol{k}'|/2}}{\sqrt{2(2\pi)^n|\boldsymbol{k}'|}} \langle 0|\, \hat{a}^\dagger_{\boldsymbol{k}} \hat{a}_{\boldsymbol{k}'}\, |0\rangle\, e^{\mathrm{i}(|\boldsymbol{k}|t - \boldsymbol{k}\cdot\boldsymbol{x})} e^{-\mathrm{i}(|\boldsymbol{k}'|t'-\boldsymbol{k}'\cdot\boldsymbol{x}')}. \tag{3.20}$$

Since $\langle 0|\, \hat{a}^\dagger_{\boldsymbol{k}} \hat{a}_{\boldsymbol{k}'}\, |0\rangle = \delta_{\boldsymbol{k},\boldsymbol{k}'}$, then

$$W^{\hat{\phi}}(t,\boldsymbol{x},t',\boldsymbol{x}') = \int \mathrm{d}^n\boldsymbol{k}\, \frac{e^{\mathrm{i}(|\boldsymbol{k}|(t'-t) - \boldsymbol{k}\cdot(\boldsymbol{x}'-\boldsymbol{x})) - |\boldsymbol{k}|\epsilon}}{2(2\pi)^n|\boldsymbol{k}|}. \tag{3.21}$$

Particularizing to 3+1 dimensions, the two-point function becomes

$$W^{\hat{\phi}}(t,\boldsymbol{x},t',\boldsymbol{x}') = \frac{1}{4\pi^2(\boldsymbol{x}-\boldsymbol{x}')^2 - (t-t'-\mathrm{i}\epsilon)^2}. \tag{3.22}$$

Note here that we see ϵ takes the form of the usual pole prescription for the Wightman function.

3.1.0.1 ϵ-regularization as a soft UV cutoff

Typically, the introduction of ϵ in Eq. (3.18) could be associated with a regularization procedure that leads to the usual pole prescription, in which the limit $\epsilon \to 0$ is well-defined and eventually taken when evaluating observable quantities. However ϵ can also be viewed as an *ad hoc* screening of the detector's sensitivity to high frequency modes of the field (i.e. a soft UV cutoff). This would effectively model, for example, a frequency dependent coupling strength where a detector does not couple to frequencies much larger than ϵ^{-1}. When giving this kind of interpretation to the ϵ-regularization one should be careful with possible non-localities introduced in the theory due to a finite value of ϵ [57]. Although this point will not be relevant when the limit $\epsilon \to 0$ is well defined, it must be taken into account when managing possibly UV divergent terms, especially in the case of the quadratic coupling Eq. (2.14), as we will see in section 3.2.

Dimensionless variable	Expression	Physical meaning
α	ΩT	Energy gap
η	ϵT	UV cutoff
β	$\lvert \boldsymbol{x}_{\mathrm{A}} - \boldsymbol{x}_{\mathrm{B}} \rvert / T$	Detectors' separation
γ_ν	$t_\nu T$	switch-on times
δ	σ / T	Detectors' size

Table 3.1: Collection of all the dimensionless quantities that are used throughout this paper.

3.1.1 Single detector contribution

The VEP is the probability of excitation of a single UDW detector initialized in its ground state in the vacuum. We briefly review how to find a general expression for the VEP of a single detector, given the two-detector state, for the usual linear UDW detector model. Then, we will calculate the VEP in 3+1 dimensions for a Gaussian switching function and spatial profile in section 3.1.1.1.

To find the time evolved state of a single detector, we begin with the bi-partite density matrix Eq. (3.12), then set $\lambda_{\mathrm{B}} = 0$. It is then simple to trace out detector B to find the single-detector reduced state,

$$\hat{\rho}_{\mathrm{A},T} = \mathrm{Tr}_{\mathrm{B}} \left(\hat{\rho}_{\mathrm{AB},T} \right) = \begin{pmatrix} 1 - \mathcal{L}_{\mathrm{AA}} & 0 \\ 0 & \mathcal{L}_{\mathrm{AA}} \end{pmatrix} + \mathcal{O}(\lambda_{\mathrm{A}}^4), \tag{3.23}$$

in the basis $|g_{\mathrm{A}}\rangle = (1,0)^\dagger$, $|e_{\mathrm{A}}\rangle = (0,1)^\dagger$. The element $\mathcal{L}_{\mathrm{AA}}$ of Eq. (3.23) is the VEP of detector A, and it is equivalent to $\mathcal{L}_{\mu\nu}$ in Eq. (3.14) when $\mu = \nu = A$,

$$\mathcal{L}_{\mathrm{AA}}{}^{\hat{\phi}} = \lambda_\nu \lambda_\nu \int_{-\infty}^{\infty} \mathrm{d}t \int_{-\infty}^{\infty} \mathrm{d}t' \int \mathrm{d}^n \boldsymbol{x} \int \mathrm{d}^n \boldsymbol{x}' \, L_{\mathrm{A}}^*(t, \boldsymbol{x}) \, L_{\mathrm{A}}(t', \boldsymbol{x}') \, W^{\hat{\phi}}(t, \boldsymbol{x}, t', \boldsymbol{x}'), \tag{3.24}$$

where $L_\nu(t', \boldsymbol{x}')$ is precisely Eq. (3.15),

$$L_\nu(t, \boldsymbol{x}) = \chi_\nu(t - t_\nu) \, F_\nu(\boldsymbol{x} - \boldsymbol{x}_\nu) \, e^{\mathrm{i}\Omega_\nu t}.$$

As expressed, $\mathcal{L}_{\mathrm{AA}}$ it is quite general and can be particularized to any spacetime dimensionality, switching function and spatial profile.

3.1.1.1 Calculation of $\mathcal{L}^{\hat{\phi}}$

For this analysis we will use a smooth switching function and spatial smearing function that are only strongly supported in finite regions in time and space (T and σ respectively).

Smooth switching and smearing will ensure the removal of all regularizable divergences of the kind studied in [93]. In particular, we choose Gaussian switching and Gaussian smearing,

$$F_\nu(\boldsymbol{x}-\boldsymbol{x}_\nu)=\frac{1}{(\sqrt{\pi}\sigma)^n}e^{-(\boldsymbol{x}-\boldsymbol{x}_\nu)^2/\sigma^2}, \tag{3.25}$$

$$\chi_\nu(t-t_\nu)=e^{-(t-t_\nu)^2/T^2}. \tag{3.26}$$

As mentioned previously, in the literature UDW detectors are often considered to be point-like. Notice that the Gaussian spatial profile can be particularized to the point-like case by taking the limit $\sigma \to 0$.

The VEP for a single linearly-coupled, 3+1 dimensional UDW detector with Gaussian switching and smearing functions is given by Eq. (3.24) with substitutions made for $W^{\hat{\phi}}(t,\boldsymbol{x},t',\boldsymbol{x}')$, $\chi_\nu(t-t_\nu)$ and $F_\nu(\boldsymbol{x}-\boldsymbol{x}_\nu)$. We substitute these functions with 3+1 dimensional Wightman function Eq. (3.22), the switching function Eq. (3.26), and the spatial profile Eq. (3.25), respectively. Furthermore, to further simplify the calculation, we apply the change of coordinates

$$\begin{aligned} u&=t_1+t_2, & v&=t_1-t_2,\\ \boldsymbol{p}&=\boldsymbol{x}_1+\boldsymbol{x}_2, & \boldsymbol{q}&=\boldsymbol{x}_1-\boldsymbol{x}_2. \end{aligned} \tag{3.27}$$

This results in

$$\mathcal{L}^{\hat{\phi}}{}_{\text{AA}}=\frac{\lambda^2}{64\pi^5\sigma^6}\int_{-\infty}^{\infty}\mathrm{d}u\, e^{-\frac{u^2}{2T^2}}\int \mathrm{d}^3\boldsymbol{p}\, e^{-\frac{\boldsymbol{p}^2}{2\sigma^2}}\int_{-\infty}^{\infty}\mathrm{d}v\int \mathrm{d}^3\boldsymbol{q}\,\frac{e^{-\frac{\boldsymbol{q}^2}{2\sigma^2}-\frac{v^2}{2T^2}-\mathrm{i}v\Omega}}{(\boldsymbol{q}^2-(v-\mathrm{i}\epsilon)^2)}. \tag{3.28}$$

The above integrals in u, $\boldsymbol{p}$ and the angular parts of $\boldsymbol{q}$ can be easily evaluated in closed form.

Taking a closer look a the integral over v, we see that the convolution theorem can be used to compute the integral over v

$$f_1 \coloneqq \int_{-\infty}^{\infty}\mathrm{d}v\,\frac{e^{v\frac{(t_\text{A}-t_\text{B})}{T^2}-\frac{v^2}{2T^2}-\mathrm{i}v\Omega}}{(q^2-(v-\mathrm{i}\epsilon)^2)}. \tag{3.29}$$

Some notation will help to find a closed form for Eq. (3.29). $\mathcal{F}$ denotes the Fourier transform

$$\mathcal{F}\big[\,g\,(x)\,\big]\,(\Omega)\;\coloneqq\int_{-\infty}^{\infty}\mathrm{d}x\,g\,(x)\,e^{\mathrm{i}\Omega x}, \tag{3.30}$$

and $*$ will be used to denote the convolution product, defined as

$$[g(x)*h(x)]\,[x]\;\coloneqq\frac{1}{2\pi}\int_{-\infty}^{\infty}\mathrm{d}\tau\,g(\tau)h\,(x-\tau). \tag{3.31}$$

The convolution theorem allows us to write f_1 in Eq. (3.29) as

$$f_1 = \mathcal{F}\big[\, g\,(v)\,\big]\,(\Omega) * \mathcal{F}\big[\, h_1\,(v)\,\big]\,(\Omega)\,, \tag{3.32}$$

where g and h_1 are functions defined as

$$g(v) \coloneqq e^{v\frac{(t_\mathrm{A}-t_\mathrm{B})}{T^2}-\frac{v^2}{2T^2}} \tag{3.33}$$

$$h_1(v) \coloneqq \frac{1}{(q^2-(v-\mathrm{i}\epsilon)^2)}\,. \tag{3.34}$$

The Fourier transforms of $g(v)$ and $h_1(v)$ are

$$\mathcal{F}\big[\, g\,(v)\,\big]\,(\Omega) = \sqrt{2\pi}Te^{\frac{\left(\mathrm{i}T^2\Omega-t_\mathrm{A}+t_\mathrm{B}\right)^2}{2T^2}} \tag{3.35}$$

$$\begin{aligned}\mathcal{F}\big[\, h_1\,(v)\,\big]\,(\Omega) = &-\frac{\mathrm{i}\pi e^{\Omega(\epsilon-\mathrm{i}q)}}{2q}\Big[2\,\mathrm{sgn}(\mathrm{Im}(q)+\epsilon)\theta(-\Omega\,\mathrm{sgn}(\epsilon+\mathrm{Im}(q)))\\ &+\mathrm{sgn}(\Omega)\left(-e^{2\mathrm{i}q\Omega}\,\mathrm{sgn}(|\epsilon-\mathrm{Im}(q)|)+\mathrm{sgn}(|\epsilon+\mathrm{Im}(q)|)+e^{2\mathrm{i}q\Omega}-1\right)\\ &-2e^{2\mathrm{i}q\Omega}\,\mathrm{sgn}(\epsilon-\mathrm{Im}(q))\theta(-\Omega\,\mathrm{sgn}(\epsilon-\mathrm{Im}(q)))\Big]\end{aligned} \tag{3.36}$$

Thus, after convolution (Eq. (3.32)) we find that f_1 takes the closed form

$$\begin{aligned}f_1 = &\left[\left(\mathrm{erfi}\left(\frac{q-\mathrm{i}\left(T^2\Omega-\mathrm{i}t_\mathrm{B}+\epsilon\right)+t_\mathrm{A}}{\sqrt{2}T}\right)+\mathrm{i}\right)e^{-\frac{2qt_\mathrm{A}}{T^2}+\frac{2qt_\mathrm{B}}{T^2}+\frac{2\mathrm{i}q\epsilon}{T^2}+2\mathrm{i}q\Omega}\right.\\ &\left.+\,\mathrm{erfi}\left(\frac{q+\mathrm{i}\left(T^2\Omega+\epsilon\right)-t_\mathrm{A}+t_\mathrm{B}}{\sqrt{2}T}\right)-\mathrm{i}\right]\frac{\pi}{2q}e^{-\frac{q^2}{2T^2}+\frac{qt_\mathrm{A}}{T^2}-\frac{qt_\mathrm{B}}{T^2}-\frac{\mathrm{i}q\epsilon}{T^2}-\mathrm{i}q\Omega+\frac{\mathrm{i}t_\mathrm{A}\epsilon}{T^2}-\frac{\mathrm{i}t_\mathrm{B}\epsilon}{T^2}+\frac{\epsilon^2}{2T^2}+\Omega\epsilon},\end{aligned} \tag{3.37}$$

where erfi is the imaginary error function, defined in terms of the error function erf, as

$$\mathrm{erfi}(z) \coloneqq -\mathrm{i}\,\mathrm{erf}(\mathrm{i}z) \tag{3.38}$$

$$\mathrm{erf}\,(z) \coloneqq \frac{2}{\sqrt{\pi}}\int_0^z \mathrm{d}t e^{-t^2}. \tag{3.39}$$

At this point, it is convenient to continue to follow notation in [36] and rewrite the result of the calculation in terms of dimensionless parameters $\alpha, \beta, \gamma, \delta, and \eta$ as outlined in Table 3.1 on page 14. After this process, Eq. (3.28) can be simplified to:

$$\begin{aligned}\mathcal{L}^{\hat{\phi}}{}_{\mathrm{AA}} = &-\frac{\lambda^2\mathrm{i}}{8\pi\delta^3}\int_0^\infty \mathrm{d}\xi\,\xi e^{\alpha\eta-\mathrm{i}\alpha\xi-\frac{\xi^2}{2\delta^2}+\frac{\eta^2}{2}-\mathrm{i}\eta\xi-\frac{\xi^2}{2}}\\ &\times\left[\mathrm{erfc}\left(\frac{\alpha+\eta-\mathrm{i}\xi}{\sqrt{2}}\right)-e^{2\mathrm{i}\xi(\alpha+\eta)}\mathrm{erfc}\left(\frac{\alpha+\eta+\mathrm{i}\xi}{\sqrt{2}}\right)\right],\end{aligned} \tag{3.40}$$

where ξ is a dummy variable of integration and erfc is the complementary error function, defined in terms of the error function (Eq. (3.39)), as follows:

$$\operatorname{erfc}(z) \coloneqq 1 - \operatorname{erf}(z). \tag{3.41}$$

The expression Eq. (3.40) depends on an arbitrary cutoff parameter η. We can take the UV cutoff scale to infinity ($\epsilon \to 0$, or in dimensionless quantities, $\eta \to 0$, as per Table 3.1 on page 14). The result is

$$\lim_{\eta\to 0}\hat{\mathcal{L}^{\phi}}_{\mathrm{AA}} = \frac{-\mathrm{i}\lambda^2}{8\pi\delta^3}\int_0^\infty \mathrm{d}\xi\, \xi e^{-\frac{\xi\left(2\mathrm{i}\alpha\delta^2+\delta^2\xi+\xi\right)}{2\delta^2}}\left[\operatorname{erfc}\left(\frac{\alpha-\mathrm{i}\xi}{\sqrt{2}}\right) - e^{2\mathrm{i}\alpha\xi}\operatorname{erfc}\left(\frac{\alpha+\mathrm{i}\xi}{\sqrt{2}}\right)\right], \tag{3.42}$$

which is not divergent. Fig. 3.1.(a) illustrates the behaviour of $\hat{\mathcal{L}^{\phi}}_{\mathrm{AA}}$ as $\eta \to 0$ is reached.

3.1.2 Multi-detector contributions

The VEP does not provide full information about the time evolution of a pair of particle detectors coupled to the field. Indeed, to characterize more complicated effects, such as entanglement harvesting [33,34,36], or quantum communication [50,57,59,60,92,96,98], the full time-evolved density matrix of two detectors coupled to the field is necessary. The detectors' time-evolved density matrix Eq. (3.12) has extra terms in addition to the VEP. Two different kinds of non-local terms, $\mathcal{L}_{\mathrm{AB}}$ and $\mathcal{M}$, now appear along with their complex conjugates. To fully characterize the two detector system, we need to find explicit expressions for these terms and study the regularity of their behaviour.

As we will discuss in detail below (and as mentioned in [36]), $\mathcal{L}_{\mathrm{AB}}$ is the term responsible for the leading order contribution to total correlations between the detectors, whereas $\mathcal{M}$ can be thought of as responsible for the harvested entanglement from the field to the detectors, as we will discuss in section 3.5.1. We will analyze these two terms independently in the next two subsections.

3.1.2.1 Calculation of $\hat{\mathcal{L}^{\phi}}_{\mathbf{AB}}$

Here we will find $\hat{\mathcal{L}_{\mathrm{AB}}{}^{\phi}}$ for linearly coupled UDW detector pairs with identical Gaussian switching functions and spatial smearings in 3+1 dimensions. We start with Eq. (3.14) and set $\nu = \mathrm{A}$ and $\mu = \mathrm{B}$. Then we make substitutions for $W^{\hat{\phi}}(t, \boldsymbol{x}, t', \boldsymbol{x}')$, $\chi_\nu(t - t_\nu)$ and $F_\nu(\boldsymbol{x} - \boldsymbol{x}_\nu)$. In particular, we use the Wightman function in 3+1 dimensions Eq. (3.22), the Gaussian spatial profile Eq. (3.25), and the Gaussian switching function Eq. (3.26) in equation Eq. (3.14). The same change of coordinates as in the calculation of $\hat{\mathcal{L}_{\mathrm{AA}}{}^{\phi}}$,

shown in Eq. (3.27), again simplifies the calculation. This transformation yields

$$\mathcal{L}^{\hat{\phi}}{}_{\rm AB} = \frac{\lambda^2 e^{-\frac{t_{\rm A}^2}{T^2}-\frac{t_{\rm B}^2}{T^2}-\frac{\boldsymbol{x}_{\rm A}^2}{\sigma^2}-\frac{\boldsymbol{x}_{\rm B}^2}{\sigma^2}}}{64\pi^5\sigma^6}\int_{-\infty}^{\infty}\mathrm{d}u\, e^{\frac{t_{\rm A}u}{T^2}+\frac{t_{\rm B}u}{T^2}-\frac{u^2}{2T^2}} \times \int \mathrm{d}^3\boldsymbol{p}\, e^{-\frac{\boldsymbol{p}^2}{2\sigma^2}+\frac{\boldsymbol{p}\boldsymbol{x}_{\rm A}}{\sigma^2}+\frac{\boldsymbol{p}\boldsymbol{x}_{\rm B}}{\sigma^2}}\int_{-\infty}^{\infty}\mathrm{d}v\int \mathrm{d}^3\boldsymbol{q}\,\frac{e^{-\frac{\boldsymbol{q}^2}{2\sigma^2}+\frac{\boldsymbol{q}\boldsymbol{x}_{\rm A}}{\sigma^2}-\frac{\boldsymbol{q}\boldsymbol{x}_{\rm B}}{\sigma^2}+\frac{t_{\rm A}v}{T^2}-\frac{t_{\rm B}v}{T^2}-\frac{v^2}{2T^2}-\mathrm{i}v\Omega}}{\boldsymbol{q}^2-(v-\mathrm{i}\epsilon)^2}. \tag{3.43}$$

The integrals over u, $\boldsymbol{p}$, the angular part of $\boldsymbol{q}$, and v can be evaluated in closed form (using the same method of convolution shown in section 3.1.1.1). As before, we follow [36] and rewrite these integrals in terms of the dimensionless parameters as outlined in Table 3.1 on page 14. The result is

$$\begin{aligned}\mathcal{L}^{\hat{\phi}}{}_{\rm AB} = {}& \frac{\lambda^2 e^{-\frac{\beta^2}{2\delta^2}-\frac{1}{2}(\gamma_{\rm A}-\gamma_{\rm B})^2}e^{\alpha\eta+\mathrm{i}\gamma_{\rm A}\eta-\mathrm{i}\gamma_{\rm B}\eta+\frac{\eta^2}{2}}}{8\pi\delta\beta}\int_0^{\infty}\mathrm{d}\xi\sinh\left(\frac{\xi\beta}{\delta^2}\right)\Bigg[\mathrm{i}\left(e^{2\xi(\mathrm{i}\alpha+\gamma_{\rm B}+\mathrm{i}\eta)}-e^{2\gamma_{\rm A}\xi}\right)\\ &+e^{2\xi(\mathrm{i}\alpha+\gamma_{\rm B}+\mathrm{i}\eta)}\mathrm{erfi}\left(\frac{-\mathrm{i}\alpha+\gamma_{\rm A}-\gamma_{\rm B}-\mathrm{i}\eta+\xi}{\sqrt{2}}\right)+e^{2\gamma_{\rm A}\xi}\mathrm{erfi}\left(\frac{\mathrm{i}\alpha-\gamma_{\rm A}+\gamma_{\rm B}+\mathrm{i}\eta+\xi}{\sqrt{2}}\right)\Bigg]\\ &\times e^{-\mathrm{i}\alpha\xi-\gamma_{\rm A}\xi-\gamma_{\rm B}\xi-\frac{\xi^2}{2\delta^2}-\mathrm{i}\eta\xi-\frac{\xi^2}{2}},\end{aligned} \tag{3.44}$$

where ξ is a dummy variable of integration. Eq. (3.44) has a well-defined limit as $\eta \to 0$,

$$\begin{aligned}\lim_{\eta\to 0}\mathcal{L}^{\hat{\phi}}{}_{\rm AB} = {}& \frac{\mathrm{i}\lambda^2 e^{-\frac{\beta^2}{2\delta^2}-\frac{1}{2}(\gamma_{\rm A}-\gamma_{\rm B})^2}}{8\pi\delta\,|\beta|}\int_0^{\infty}\mathrm{d}\xi\sinh\left(\frac{\xi\,|\beta|}{\delta^2}\right)e^{-\mathrm{i}\alpha\xi-\gamma_{\rm A}\xi-\gamma_{\rm B}\xi-\frac{\xi^2}{2\delta^2}-\frac{\xi^2}{2}}\\ &\times\left[e^{2\xi(\gamma_{\rm B}+\mathrm{i}\alpha)}\mathrm{erfc}\left(\frac{\alpha+\mathrm{i}(\gamma_{\rm A}-\gamma_{\rm B}+\xi)}{\sqrt{2}}\right)-e^{2\gamma_{\rm A}\xi}\mathrm{erfc}\left(\frac{\alpha+\mathrm{i}(\gamma_{\rm A}-\gamma_{\rm B}-\xi)}{\sqrt{2}}\right)\right].\end{aligned} \tag{3.45}$$

Not only is the integrand well-defined, but the integral is convergent as well. We show numerically how the convergent limit $\eta \to 0$ of $|\mathcal{L}^{\hat{\phi}}{}_{\rm AB}|$ is reached in Fig. 3.1.(b).

3.1.2.2 Calculation of $\mathcal{M}^{\hat{\phi}}$

In the following, we will derive $\mathcal{M}^{\hat{\phi}}$ for a pair of quadratically coupled UDW detectors with identical Gaussian switching functions and spatial profiles in 3+1 dimensions. We begin with Eq. (3.13) and make the appropriate substitutions: we substitute into Eq. (3.13) the Wightman function in 3+1 dimensions Eq. (3.22), the spatial profile Eq. (3.25), and the switching function Eq. (3.26). The integrals take a particularly simple form under the same change of coordinates Eq. (3.27) as in both previous calculations. In the case of $\mathcal{M}^{\hat{\phi}}$, this change of coordinates also helps to de-nest the nested

time integrals. This yields

$$\mathcal{M}^{\hat{\phi}} = -e^{-\frac{t_{\rm A}^2}{T^2}-\frac{t_{\rm B}^2}{T^2}-\frac{\boldsymbol{x}_{\rm A}^2}{\sigma^2}-\frac{\boldsymbol{x}_{\rm B}^2}{\sigma^2}} \int \mathrm{d}^3\boldsymbol{p}\, e^{-\frac{p^2}{2\sigma^2}} \int_{-\infty}^{\infty}\mathrm{d}u\, e^{+\frac{t_{\rm A}u}{T^2}+\frac{t_{\rm B}u}{T^2}-\frac{u^2}{2T^2}+\mathrm{i}u\Omega} \tag{3.46}$$
$$\times \int \mathrm{d}^3\boldsymbol{q} \int_{-\infty}^{\infty}\mathrm{d}v\, e^{-\frac{v^2}{2T^2}} e^{-\frac{q^2}{2\sigma^2}} \left[\frac{\lambda^2 e^{-\frac{q\boldsymbol{x}_{\rm A}}{\sigma^2}+\frac{q\boldsymbol{x}_{\rm B}}{\sigma^2}-\frac{t_{\rm A}v}{T^2}+\frac{t_{\rm B}v}{T^2}}}{64\pi^5\sigma^6\left(q^2-(v-\mathrm{i}\epsilon)^2\right)} + \frac{\lambda^2 e^{-(-\frac{q\boldsymbol{x}_{\rm A}}{\sigma^2}+\frac{q\boldsymbol{x}_{\rm B}}{\sigma^2}-\frac{t_{\rm A}v}{T^2}+\frac{t_{\rm B}v}{T^2})}}{64\pi^5\sigma^6\left(q^2-(v-\mathrm{i}\epsilon)^2\right)}\right],$$

The integrals in u, $\boldsymbol{p}$, and the angular parts of $\boldsymbol{q}$ can be evaluated in closed form. This results in

$$\mathcal{M}^{\hat{\phi}} = e^{-\frac{t_{\rm A}^2}{2T^2}+\frac{t_{\rm A}t_{\rm B}}{T^2}-\frac{t_{\rm B}^2}{2T^2}-\frac{T^2\Omega^2}{2}+\mathrm{i}t_{\rm A}\Omega+\mathrm{i}t_{\rm B}\Omega-\frac{\boldsymbol{x}_{\rm A}^2}{2\sigma^2}+\frac{\boldsymbol{x}_{\rm A}\boldsymbol{x}_{\rm B}}{\sigma^2}-\frac{\boldsymbol{x}_{\rm B}^2}{2\sigma^2}} \frac{\lambda^2 T}{2\pi^2\sigma(\boldsymbol{x}_{\rm A}-\boldsymbol{x}_{\rm B})} \tag{3.47}$$
$$\times \int_{-\infty}^{\infty}\mathrm{d}v \int_0^{\infty}\mathrm{d}q\, \frac{e^{-\frac{q^2}{2\sigma^2}-\frac{v^2}{2T^2}}q}{(-q^2+(v-\mathrm{i}\epsilon)^2)} \sinh\left(\frac{q(\boldsymbol{x}_{\rm A}-\boldsymbol{x}_{\rm B})}{\sigma^2}\right)\cosh\left(\frac{v(t_{\rm A}-t_{\rm B})}{T^2}\right).$$

To obtain a closed form for the integral over v, we simplify $\mathcal{M}^{\hat{\phi}}$ by choosing to switch on the detectors simultaneously within their co-moving frame, i.e. we make the simplifying additional assumption $t_{\rm A}-t_{\rm B}=0$. Then, $\mathcal{M}^{\hat{\phi}}$ (in dimensionless parameters as shown in 3.1 on page 14) takes the form

$$\begin{aligned}\mathcal{M}^{\hat{\phi}}{}_{t_{\rm A}=t_{\rm B}} = &-\frac{\lambda^2}{16\pi^2\delta\beta}\int_0^{\infty}\mathrm{d}q \sinh\left(\frac{\xi\beta}{\delta^2}\right)\Bigg[\Bigg[2\pi\,\mathrm{erfi}\left(\frac{\xi T-\mathrm{i}\eta T}{\sqrt{2}T}\right)-2\,\mathrm{Ei}\left(\frac{(T\xi-\mathrm{i}T\eta)^2}{2T^2}\right)\\ &+\log\left(\frac{(\xi T-\mathrm{i}\eta T)^2}{T^2}\right)-\log\left(\frac{T^2}{(\xi T-\mathrm{i}\eta T)^2}\right)-4\log(\xi T-\mathrm{i}\eta T)+4\log(T)\Bigg]e^{-\frac{(\xi T-\mathrm{i}\eta T)^2}{2T^2}}\\ &+e^{-\frac{(\xi T+\mathrm{i}\eta T)^2}{2T^2}}\Bigg[2\pi\,\mathrm{erfi}\left(\frac{\xi T+\mathrm{i}\eta T}{\sqrt{2}T}\right)+2\,\mathrm{Ei}\left(\frac{(\mathrm{i}T\eta+T\xi)^2}{2T^2}\right)+\log\left(\frac{1}{(\xi T+\mathrm{i}\eta T)^2}\right)\\ &+4\log(-\xi T-\mathrm{i}\eta T)-2\log(\xi T+\mathrm{i}\eta T)\Bigg]\Bigg]e^{-\frac{\alpha^2\delta^2T^2-4\mathrm{i}\alpha\gamma_{\rm A}\delta^2T^2+\beta^2T^2+\xi^2T^2}{2\delta^2T^2}},\end{aligned} \tag{3.48}$$

where ξ is a dummy variable of integration and $\mathrm{Ei}(z)$ is the principal value of the exponential integral function defined as

$$\mathrm{Ei}(z) \coloneqq -\,\mathrm{P.V.}\int_{-z}^{\infty}\mathrm{d}t\,\frac{e^{-t}}{t}. \tag{3.49}$$

$\mathcal{M}^{\hat{\phi}}$ is well behaved in the UV limit. If we remove the cutoff, taking the limit $\epsilon\to 0$ (i.e. , $\eta\to 0$), we obtain

$$\lim_{\eta\to 0}\mathcal{M}^{\hat{\phi}}{}_{t_{\rm A}=t_{\rm B}} = -\frac{\lambda^2 e^{-\frac{\alpha^2}{2}+2\mathrm{i}\alpha\gamma_{\rm A}-\frac{\beta^2}{2\delta^2}}}{4\pi\delta\beta}\int_0^{\infty}\mathrm{d}\xi\, e^{-\frac{\xi^2}{2\delta^2}-\frac{\xi^2}{2}}\,\mathrm{i}\,\mathrm{erfc}\left(\frac{\mathrm{i}\xi}{\sqrt{2}}\right)\sinh\left(\frac{\xi(\beta)}{\delta^2}\right). \tag{3.50}$$

The integral is convergent, and how the limit is reached as $\eta\to 0$ is shown in Fig. 3.1.(c).

3.1.2.3 Momentum representation versus position representation

We note that in previous literature closed expressions for Eq. (3.42), Eq. (3.45), and Eq. (3.50) were found for Gaussian switching and smearing functions in 3+1 dimensions by working in the momentum representation [36]. By contrast, here we have worked in the position representation. One can readily check numerically that $\lim_{\eta\to 0}\mathcal{L}_{\mu\nu}{}^{\hat{\phi}}$ (Eq. (3.42) and Eq. (3.45)) and $\lim_{\eta\to 0}\mathcal{M}^{\hat{\phi}}$ (Eq. (3.50)) are equivalent to those in [36]. While working in position representation complicates the final expressions Eq. (3.42), Eq. (3.45), and Eq. (3.50), we found that the equivalent expressions for the detector coupled quadratically to the salar field (Eq. (3.81), Eq. (3.84), and Eq. (3.86)) require the position representation for numerical stability. Moreover, there is an additional advantage working in the position representation in the linear case: the method of computing leading order density matrix elements in the position representation used here yields results that have greater numerical stability for small detector gap in those terms for which we do not have closed expressions, neither in position nor in momentum representation in [36], as we will show when we present numerical results in section 3.5.

3.2 Nonlinear Unruh-DeWitt detector

Quadratic single-detector UDW models (such as the quadratic scalar model introduced by Hinton in [39], the cavity detector coupled to a fermionic field [55], or the fermionic UDW-like detector model introduced in [37, 38]) have a VEP that presents persistent divergences (not removable with a smooth switching and/or smearing as in the linear case, see 2.4.0.1). However, the persistent divergences in the single detector model can be renormalized with techniques analogous to those used in QED to renormalize tadpole diagrams [40]. Once renormalized, the quadratically coupled single-detector UDW model is regularizable both in its scalar and fermionic variants.

The renormalized, quadratic UDW Hamiltonian for two detectors is

$$\hat{H}^{\hat{\phi}^2}=\sum_{\nu\in\{\mathrm{A,B}\}}\lambda_\nu\chi_\nu(t-t_\nu)\hat{\mu}_\nu(t)\int \mathrm{d}^n\boldsymbol{x}\,F_\nu(\boldsymbol{x}-\boldsymbol{x}_\nu):\hat{\phi}^2(\boldsymbol{x},t):, \tag{3.51}$$

where $\nu\in\{\mathrm{A,B}\}$ is the label identifying detectors A and B. Note that the coupling strength in the quadratic case does not have the same dimensions as in the linear case.

Following section 3.1, one finds that the time evolved bipartite state of two detectors interacting through a quadratic coupling in the field, initially uncorrelated in their ground state,

$$\hat{\rho}_{\mathrm{AB},0}=|g_{\mathrm{A}}\rangle\langle g_{\mathrm{A}}|\otimes|g_{\mathrm{B}}\rangle\langle g_{\mathrm{B}}|\,, \tag{3.52}$$

takes the same form as with the linear detector model:

$$\hat{\rho}_{\mathrm{AB,T}} = \begin{pmatrix} 1-\mathcal{L}_{\mathrm{AA}}-\mathcal{L}_{\mathrm{BB}} & 0 & 0 & \mathcal{M}^* \\ 0 & \mathcal{L}_{\mathrm{AA}} & \mathcal{L}_{\mathrm{AB}} & 0 \\ 0 & \mathcal{L}_{\mathrm{BA}} & \mathcal{L}_{\mathrm{BB}} & 0 \\ \mathcal{M} & 0 & 0 & 0 \end{pmatrix} + \mathcal{O}(\lambda_\nu^4), \tag{3.53}$$

where $\mathcal{M}$ and $\mathcal{L}_{\mu\nu}$ are

$$\mathcal{M}^{\hat{\phi}^2} = -\lambda_{\mathrm{A}}\lambda_{\mathrm{B}} \int_{-\infty}^{\infty} \mathrm{d}t \int_{-\infty}^{t} \mathrm{d}t' \int \mathrm{d}^n\boldsymbol{x} \int \mathrm{d}^n\boldsymbol{x}'\, M(t,\boldsymbol{x},t',\boldsymbol{x}')\, W^{\hat{\phi}^2}(t,\boldsymbol{x},t',\boldsymbol{x}') \tag{3.54}$$

$$\mathcal{L}^{\hat{\phi}^2}{}_{\nu\mu} = \lambda_\nu\lambda_\mu \int_{-\infty}^{\infty} \mathrm{d}t \int_{-\infty}^{\infty} \mathrm{d}t' \int \mathrm{d}^n\boldsymbol{x} \int \mathrm{d}^n\boldsymbol{x}'\, L_\nu^*(t,\boldsymbol{x})\, L_\mu(t',\boldsymbol{x}')\, W^{\hat{\phi}^2}(t,\boldsymbol{x},t'.\boldsymbol{x}'), \tag{3.55}$$

where the superscript $\hat{\phi}^2$ denotes quadratic coupling to the real scalar field and $W^{\hat{\phi}^2}$ is the two-point correlator of the normal ordered field operator, $:\hat{\phi}^2:$. Explicitly,

$$W^{\hat{\phi}^2}(t,\boldsymbol{x},t',\boldsymbol{x}') = \langle 0| :\hat{\phi}^2(\boldsymbol{x},t): :\hat{\phi}^2(\boldsymbol{x}',t'): |0\rangle\,. \tag{3.56}$$

These matrix elements are structurally analagous to the those in the linearly coupled detector, Eqs. Eq. (3.14) and Eq. (3.13). Indeed, M and L_ν are also defined as in Eqs. Eq. (3.16) and Eq. (3.15), respectively.

In what follows, we will illustrate the relationship between the Wightman functional of th linear model, $W^{\hat{\phi}}$ (Eq. (3.17)), and the equivalent function for the quadratic model, $W^{\hat{\phi}^2}$. We start with the relationship between an operator $\hat{A}$ and its normal ordered version:

$$:\hat{A}: = \hat{A} - \langle 0|\,\hat{A}\,|0\rangle\,. \tag{3.57}$$

Using this identity, $W^{\hat{\phi}^2}$ can be rewritten as

$$W^{\hat{\phi}^2}(t,\boldsymbol{x},t',\boldsymbol{x}') = \langle 0|\,\hat{\phi}^2(t,\boldsymbol{x})\hat{\phi}^2(t',\boldsymbol{x}')\,|0\rangle - \langle 0|\,\hat{\phi}^2(t,\boldsymbol{x})\,|0\rangle\,\langle 0|\,\hat{\phi}^2(t',\boldsymbol{x}')\,|0\rangle\,. \tag{3.58}$$

The first term of $W^{\hat{\phi}^2}(t,\boldsymbol{x},t',\boldsymbol{x}')$ can be simplified. To do so, we will write the field operator as $\hat{\phi} = \hat{\phi}^+ + \hat{\phi}^-$, where $\hat{\phi}^+$ and $\hat{\phi}^-$ are defined as

$$\hat{\phi}^+(\boldsymbol{x},t) = \int \frac{\mathrm{d}^n\boldsymbol{k}\, e^{-\epsilon|\boldsymbol{k}|/2}}{\sqrt{2(2\pi)^n|\boldsymbol{k}|}}\, \hat{a}_k^\dagger\, e^{\mathrm{i}(|\boldsymbol{k}|t-\boldsymbol{k}\cdot\boldsymbol{x})} \qquad \hat{\phi}^-(\boldsymbol{x},t) = \int \frac{\mathrm{d}^n\boldsymbol{k}\, e^{-\epsilon|\boldsymbol{k}|/2}}{\sqrt{2(2\pi)^n|\boldsymbol{k}|}}\, \hat{a}_k\, e^{-\mathrm{i}(|\boldsymbol{k}|t-\boldsymbol{k}\cdot\boldsymbol{x})} \tag{3.59}$$

which satisfy the commutation relation

$$\left[\hat{\phi}^-(\boldsymbol{x}_\mu,t_\mu), \hat{\phi}^+(\boldsymbol{x}_\nu,t_\nu)\right] = \mathcal{C}_{\mu\nu}\mathbb{1} \tag{3.60}$$

where $\mathcal{C}_{\mu\nu} \in \mathbb{C}$ is given by

$$\mathcal{C}_{\mu\nu} = \int \frac{\mathrm{d}^n \boldsymbol{k}\, e^{-\epsilon|\boldsymbol{k}|/2}}{2(2\pi)^n |\boldsymbol{k}|} e^{\mathrm{i}(|\boldsymbol{k}|(t_\nu - t_\mu) - \boldsymbol{k}\cdot(\boldsymbol{x}_\nu - \boldsymbol{x}_\mu))}. \tag{3.61}$$

Using the notation $\hat{\phi}_\nu \equiv \hat{\phi}(\boldsymbol{x}_\nu, t_\nu)$, a scalar field vacuum four-point function $\langle 0| \hat{\phi}_1 \hat{\phi}_2 \hat{\phi}_3 \hat{\phi}_4 |0\rangle$ can be rewritten as

$$\langle 0|\hat{\phi}_1 \hat{\phi}_2 \hat{\phi}_3 \hat{\phi}_4 |0\rangle = \langle 0| \hat{\phi}_1^- \hat{\phi}_2^- \hat{\phi}_3^+ \hat{\phi}_4^+ |0\rangle + \langle 0| \hat{\phi}_1^- \hat{\phi}_2^+ \hat{\phi}_3^- \hat{\phi}_4^+ |0\rangle , \tag{3.62}$$

where, to remove all vanishing summands, we have used that $\hat{\phi}_\nu^- |0\rangle = \langle 0| \hat{\phi}_\nu^+ = 0$ and that only summands with as many $\hat{\phi}^+$ as $\hat{\phi}^-$ contribute to the final expression. Commuting the operators $\hat{\phi}^+$ and $\hat{\phi}^-$ (using Eq. (3.60)), we can write the first summand in Eq. (3.62) as

$$\langle 0| \hat{\phi}_1^- \hat{\phi}_2^- \hat{\phi}_3^+ \hat{\phi}_4^+ |0\rangle = \mathcal{C}_{23}\mathcal{C}_{14} + \mathcal{C}_{13}\mathcal{C}_{24} \tag{3.63}$$

and the second as

$$\langle 0| \hat{\phi}_1^- \hat{\phi}_2^+ \hat{\phi}_3^- \hat{\phi}_4^+ |0\rangle = \mathcal{C}_{12}\mathcal{C}_{34}. \tag{3.64}$$

Thus Eq. (3.62) can be written as

$$\langle 0|\hat{\phi}_1 \hat{\phi}_2 \hat{\phi}_3 \hat{\phi}_4 |0\rangle = \mathcal{C}_{23}\mathcal{C}_{14} + \mathcal{C}_{13}\mathcal{C}_{24} + \mathcal{C}_{12}\mathcal{C}_{34}. \tag{3.65}$$

From the relation (Eq. (3.60)), we see that we can rewrite the $\mathcal{C}_{\mu\nu}$ coefficients as

$$\mathcal{C}_{\mu\nu} = \langle 0| \left[\hat{\phi}_\mu^-, \hat{\phi}_\nu^+\right] |0\rangle = \langle 0| \hat{\phi}_\mu^- \hat{\phi}_\nu^+ |0\rangle = \langle 0| \hat{\phi}_\mu \hat{\phi}_\nu |0\rangle , \tag{3.66}$$

which allows us to rewrite Eq. (3.65) as

$$\begin{aligned}\langle 0| \hat{\phi}_1 \hat{\phi}_2 \hat{\phi}_3 \hat{\phi}_4 |0\rangle = &\langle 0| \hat{\phi}_1 \hat{\phi}_2 |0\rangle \langle 0| \hat{\phi}_3 \hat{\phi}_4 |0\rangle + \langle 0| \hat{\phi}_2 \hat{\phi}_3 |0\rangle \langle 0| \hat{\phi}_1 \hat{\phi}_4 |0\rangle \\ &+ \langle 0| \hat{\phi}_1 \hat{\phi}_3 |0\rangle \langle 0| \hat{\phi}_2 \hat{\phi}_4 |0\rangle .\end{aligned} \tag{3.67}$$

To apply this identity to Eq. (3.58), we set $\hat{\phi}_1 = \hat{\phi}_2 = \hat{\phi}(t, \boldsymbol{x})$ and $\hat{\phi}_3 = \hat{\phi}_4 = \hat{\phi}(t', \boldsymbol{x}')$. Then, the first summand in Eq. (3.58) becomes

$$\langle 0|\hat{\phi}^2(t, \boldsymbol{x}) \hat{\phi}^2(t', \boldsymbol{x}') |0\rangle = \langle 0| \hat{\phi}^2(t, \boldsymbol{x}) |0\rangle \langle 0| \hat{\phi}^2(t', \boldsymbol{x}') |0\rangle + 2 \left(\langle 0| \hat{\phi}(t, \boldsymbol{x}) \hat{\phi}(t', \boldsymbol{x}') |0\rangle \right)^2 . \tag{3.68}$$

This allows Eq. (3.58) to be written as

$$W^{\hat{\phi}^2}(t, \boldsymbol{x}, t', \boldsymbol{x}') = 2 \left(\langle 0| \hat{\phi}(t, \boldsymbol{x}) \hat{\phi}(t', \boldsymbol{x}') |0\rangle \right)^2 , \tag{3.69}$$

which shows the correlation functions $W^{\hat{\phi}}$ (Eq. (3.17)) and $W^{\hat{\phi}^2}$ (Eq. (3.56)) satisfy the following relation

$$W^{\hat{\phi}^2}(t,\boldsymbol{x},t',\boldsymbol{x}') = 2W^{\hat{\phi}}(t,\boldsymbol{x},t',\boldsymbol{x}')^2. \tag{3.70}$$

This relation, along with the mode-expanded linear Wightman function, Eq. (3.21),

$$W^{\hat{\phi}}(t,\boldsymbol{x},t',\boldsymbol{x}') = \int \mathrm{d}^n\boldsymbol{k}\,\frac{e^{\mathrm{i}(|\boldsymbol{k}|(t'-t)-\boldsymbol{k}\cdot(\boldsymbol{x}'-\boldsymbol{x}))-|\boldsymbol{k}|\epsilon}}{2(2\pi)^n|\boldsymbol{k}|},$$

let us write $W^{\hat{\phi}^2}$ explicitly as

$$W^{\hat{\phi}^2}(t,\boldsymbol{x},t',\boldsymbol{x}') = \int \mathrm{d}^n\boldsymbol{k}_1 \int \mathrm{d}^n\boldsymbol{k}_2 \frac{e^{\mathrm{i}((|\boldsymbol{k}_2|+|\boldsymbol{k}_1|)(t'-t)-(\boldsymbol{k}_2+\boldsymbol{k}_1)\cdot(\boldsymbol{x}'-\boldsymbol{x}))-(|\boldsymbol{k}_1|+|\boldsymbol{k}_2|)\epsilon}}{(2\pi)^{2n}|\boldsymbol{k}_1||\boldsymbol{k}_2|}. \tag{3.71}$$

If we particularize to 3+1 dimensions, the correlation function $W^{\hat{\phi}^2}$ is

$$W^{\hat{\phi}^2}(t,\boldsymbol{x},t',\boldsymbol{x}') = \frac{2}{\left[4\pi^2(\boldsymbol{x}-\boldsymbol{x'})^2-(t-t'-\mathrm{i}\epsilon)^2\right]^2}. \tag{3.72}$$

Note here that the correlator for the quadratic UDW detector has a higher power polynomial in $\boldsymbol{x}$ and t in its denominator than does the usual correlator for the linear UDW detector.

3.2.1 Single detector contribution

Here we will find a general expression for the VEP for a detector quadratically coupled to the real scalar field. Then, in section 3.2.1.1, we will particularize to 3+1 dimensions and find a general expression for the VEP for a Gaussian switching function and spatial profile.

The time evolved state of a single detector can be found by setting $\lambda_{\mathrm{B}} = 0$ in the bi-partite density matrix, then tracing out detector B. The result is exactly Eq. (3.23):

$$\hat{\rho}_{\mathrm{A},T} = \mathrm{Tr}_{\mathrm{B}}\left(\hat{\rho}_{\mathrm{AB},T}\right) = \begin{pmatrix} 1-\mathcal{L}_{\mathrm{AA}} & 0 \\ 0 & \mathcal{L}_{\mathrm{AA}} \end{pmatrix} + \mathcal{O}(\lambda_{\mathrm{A}}^4),$$

in the basis $|g_{\mathrm{A}}\rangle = (1,0)^\dagger$, $|e_{\mathrm{A}}\rangle = (0,1)^\dagger$. The element $\mathcal{L}_{\mathrm{AA}}$ of Eq. (3.23) is the VEP of detector A, and it is equivalent to $\mathcal{L}_{\mu\nu}$ in Eq. (3.14) when $\mu = \nu = A$,

$$\mathcal{L}_{\mathrm{AA}}{}^{\hat{\phi}^2} = \lambda_{\mathrm{A}}^2 \int_{-\infty}^{\infty}\mathrm{d}t \int_{-\infty}^{\infty}\mathrm{d}t' \int \mathrm{d}^n\boldsymbol{x} \int \mathrm{d}^n\boldsymbol{x}'\, L_{\mathrm{A}}^*(t,\boldsymbol{x})\, L_{\mathrm{A}}(t',\boldsymbol{x}')\, W^{\hat{\phi}^2}(t,\boldsymbol{x},t',\boldsymbol{x}'), \tag{3.73}$$

Now instead of the Wightman function, $W^{\hat{\phi}}$ as in Eq. (3.17), we have the two-point function of the normal ordered operator $:\hat{\phi}^2:$, $W^{\hat{\phi}^2}$. Although $L_\nu(t',\boldsymbol{x}')$ is still the same as Eq. (3.15),

$$L_\nu(t,\boldsymbol{x}) = \chi_\nu(t-t_\nu)\, F_\nu(\boldsymbol{x}-\boldsymbol{x}_\nu)\, e^{\mathrm{i}\Omega_\nu t}.$$

As expressed, $\mathcal{L}_{\mathrm{AA}}{}^{\hat{\phi}^2}$ is quite general and can be particularized to any spacetime dimensionality, switching function and spatial profile.

3.2.1.1 Calculation of $\mathcal{L}^{\hat{\phi}^2}$

Beginning with Eq. (3.73), we substitute the general functions $W^{\hat{\phi}^2}$, F, and χ with particular expresions, namely the quadratic two-point correlator in 3+1 dimensions Eq. (3.72), the Gaussian spatial profile Eq. (3.25), and the Gaussian switching function Eq. (3.26). Applying These substitutions the same change of coordinates as in the linear case, Eq. (3.27), yields

$$\mathcal{L}_{\mathrm{AA}}{}^{\hat{\phi}^2} = \frac{\lambda^2}{128\pi^7\sigma^6}\int_{-\infty}^{\infty}\mathrm{d}u\, e^{-\frac{u^2}{2T^2}}\int \mathrm{d}^3\boldsymbol{p}\, e^{-\frac{\boldsymbol{p}^2}{2\sigma^2}}\int_{-\infty}^{\infty}\mathrm{d}v\int \mathrm{d}^3\boldsymbol{q}\,\frac{e^{-\frac{\boldsymbol{q}^2}{2\sigma^2}-\frac{v^2}{2T^2}-\mathrm{i}v\Omega}}{\left(\boldsymbol{q}^2-(v-\mathrm{i}\epsilon)^2\right)^2}. \tag{3.74}$$

The integrals over u, $\boldsymbol{p}$, the angular part of $\boldsymbol{q}$, and v can be evaluated in closed form similarly to Eq. (3.40), where the integral over v is calculated using the convolution theorem, where now the relevant integral is

$$f_2 \coloneqq \int_{-\infty}^{\infty}\mathrm{d}v\,\frac{e^{v\frac{(t_\mathrm{A}-t_\mathrm{B})}{T^2}-\frac{v^2}{2T^2}-\mathrm{i}v\Omega}}{\left(q^2-(v-\mathrm{i}\epsilon)^2\right)^2}. \tag{3.75}$$

As before, we will let $\mathcal{F}$ denote the Fourier transform as in Eq. (3.30) and let $*$ denote the convolution product, as in Eq. (3.31). Then, the convolution theorem allows us to write f_2 in Eq. (3.75) as

$$f_2 = \mathcal{F}\big[\, g\,(v)\,\big]\,(\Omega) * \mathcal{F}\big[\, h_2\,(v)\,\big]\,(\Omega)\,, \tag{3.76}$$

where g is the same as in Eq. (3.33) and h_2 is defined as

$$h_2(v) \coloneqq \frac{1}{\left(q^2-(v-\mathrm{i}\epsilon)^2\right)^2}\,. \tag{3.77}$$

The Fourier transform of $g(v)$ is given in Eq. (3.35) and $h_2(v)$ is

$$\begin{aligned}\mathcal{F}\big[\, h_2\,(v)\,\big]\,(\Omega) = \Bigg(&\operatorname{sgn}(\Omega)\Big[e^{2\mathrm{i}q\Omega}(q\Omega+i)\operatorname{sgn}(|\epsilon-\operatorname{Im}(q)|)+(q\Omega-i)\operatorname{sgn}(|\epsilon+\operatorname{Im}(q)|)\\ &+\left(\mathrm{i}e^{2\mathrm{i}q\Omega}+q\Omega+q\Omega e^{2\mathrm{i}q\Omega}-\mathrm{i}\right)\Big]+2\Big[e^{2\mathrm{i}q\Omega}(q\Omega+i)\operatorname{sgn}(\epsilon-\operatorname{Im}(q))\theta(-\Omega\operatorname{sgn}(\epsilon-\operatorname{Im}(q)))\\ &+(q\Omega-i)\operatorname{sgn}(\operatorname{Im}(q)+\epsilon)\theta(-\Omega\operatorname{sgn}(\epsilon+\operatorname{Im}(q)))\Big]\Bigg)\frac{\pi e^{\Omega(\epsilon-\mathrm{i}q)}}{4q^3}.\end{aligned} \tag{3.78}$$

Thus, using Eq. (3.76) we find that f_2 takes the closed form

$$
\begin{aligned}
f_2 = \frac{1}{4q^3T^2} e^{-\frac{(q+\mathrm{i}\epsilon)\left(q+\mathrm{i}\left(2T^2\Omega+\epsilon\right)-2t_{\mathrm{A}}+2t_{\mathrm{B}}\right)}{2T^2}} \Bigg[\pi\Bigg(& -\mathrm{i}q^2 + qT^2\Omega + \mathrm{i}qt_{\mathrm{A}} - \mathrm{i}qt_{\mathrm{B}} + q\epsilon - \mathrm{i}T^2 \\
& + \pi\left(T^2 + q\left(q + \mathrm{i}\left(T^2\Omega+\epsilon\right) - t_{\mathrm{A}} + t_{\mathrm{B}}\right)\right)\mathrm{erfi}\left(\frac{q+\mathrm{i}\left(T^2\Omega+\epsilon\right)-t_{\mathrm{A}}+t_{\mathrm{B}}}{\sqrt{2}T}\right) \\
& - 2\sqrt{2\pi}qTe^{\frac{\left(q+\mathrm{i}\left(T^2\Omega+\epsilon\right)-t_{\mathrm{A}}+t_{\mathrm{B}}\right)^2}{2T^2}} + \Bigg[e^{\frac{2q\left(\mathrm{i}\left(T^2\Omega+\epsilon\right)-t_{\mathrm{A}}+t_{\mathrm{B}}\right)}{T^2}} \\
& \times\left(T^2 + q\left(q - \mathrm{i}\left(T^2\Omega - \mathrm{i}t_{\mathrm{B}} + \epsilon\right) + t_{\mathrm{A}}\right)\right)\left(\mathrm{erfi}\left(\frac{q-\mathrm{i}\left(T^2\Omega - \mathrm{i}t_{\mathrm{B}} + \epsilon\right)+t_{\mathrm{A}}}{\sqrt{2}T}\right)+\mathrm{i}\right)\Bigg]\Bigg)\Bigg],
\end{aligned}
\tag{3.79}
$$

which we will use, along with the convention of using the the dimensionless parameters $\alpha, \beta, \gamma, \delta, \eta$, as in [36] (see Table 3.1 on page 14), to express Eq. (3.74) in the form

$$
\begin{aligned}
\mathcal{L}_{\mathrm{AA}}{}^{\hat{\phi}^2} = & \frac{\lambda^2 e^{\alpha\eta+\frac{\eta^2}{2}}}{32\pi^4\delta^3T^3}\int_0^\infty \mathrm{d}q\, \frac{e^{-\mathrm{i}\alpha\xi-\frac{\xi^2}{2\delta^2}-\mathrm{i}\eta\xi-\frac{\xi^2}{2}}}{\xi} \\
& \times\Bigg[\pi\Bigg[\alpha\xi+\eta\xi-\mathrm{i}(\xi^2+1)+e^{2\mathrm{i}\xi(\alpha+\eta)}\left(\alpha\xi+\eta\xi+\mathrm{i}\left(\xi^2+1\right)\right)\mathrm{erfc}\left(\frac{\alpha+\eta+\mathrm{i}\xi}{\sqrt{2}}\right)\Bigg] \\
& - 2\sqrt{2\pi}\xi e^{-\frac{1}{2}(\alpha+\eta-\mathrm{i}\xi)^2} + \pi\left(\mathrm{i}\alpha\xi+\mathrm{i}\eta\xi+\xi^2+1\right)\mathrm{erfi}\left(\frac{\mathrm{i}\alpha+\mathrm{i}\eta+\xi}{\sqrt{2}}\right)\Bigg],
\end{aligned}
\tag{3.80}
$$

where ξ is a dummy integration variable. For this integrand, the limit of no cutoff, i.e, $\frac{\epsilon}{T} = \eta \to 0$, at constant T, is well-defined:

$$
\begin{aligned}
\lim_{\eta\to 0}\mathcal{L}_{\mathrm{AA}}{}^{\hat{\phi}^2} = & \frac{\lambda^2}{32\pi^4\delta^3T^2}\int_0^\infty \mathrm{d}\xi\, \frac{e^{-\frac{\alpha^2}{2}-\mathrm{i}\alpha\xi-\frac{1}{2}\left(\frac{1}{\delta^2}+1\right)\xi^2}}{\xi}\Bigg[-\mathrm{i}\pi e^{\frac{\alpha^2}{2}}\xi^2 + \pi e^{\frac{\alpha^2}{2}}\alpha\xi - \mathrm{i}\pi e^{\frac{\alpha^2}{2}} \\
& + \mathrm{i}\pi\xi^2 e^{\frac{1}{2}\alpha(\alpha+4\mathrm{i}\xi)} + \pi\alpha\xi e^{\frac{1}{2}\alpha(\alpha+4\mathrm{i}\xi)} - 2\sqrt{2\pi}\xi e^{\frac{1}{2}\xi(\xi+2\mathrm{i}\alpha)} + \mathrm{i}\pi e^{\frac{1}{2}\alpha(\alpha+4\mathrm{i}\xi)} \\
& - \pi e^{\frac{\alpha^2}{2}}\left(\alpha\xi - \mathrm{i}\left(\xi^2+1\right)\right)\mathrm{erf}\left(\frac{\alpha-\mathrm{i}\xi}{\sqrt{2}}\right) - \pi e^{\frac{1}{2}\alpha(\alpha+4\mathrm{i}\xi)}\left(\alpha\xi+\mathrm{i}\left(\xi^2+1\right)\right)\mathrm{erf}\left(\frac{\alpha+\mathrm{i}\xi}{\sqrt{2}}\right)\Bigg].
\end{aligned}
\tag{3.81}
$$

This integral is convergent. How the convergent $\eta \to 0$ limit is reached is shown numerically in Fig. 3.1.(d).

3.2.2 Multi-detector contributions

The VEP provides only partial information about the time evolution of a pair of particle detectors coupled to the field. The full time-evolved density matrix of two detectors, Eq. (3.12), has extra terms in addition to the VEP, namely $\mathcal{L}_{\mathrm{AB}}$ and $\mathcal{M}$, which are crucial for more complicated effects, such as entanglement harvesting [33, 34, 36], or quantum

communication [50, 57, 59, 60, 92, 96, 98]. To fully characterize the two detector system, we need to find explicit expressions for these terms and study the regularity of their behaviour.

As we will discuss in detail in section 3.5 (and as mentioned in [36]), the leading order contribution to classical correlations between the detectors is controlled by a combination of $\mathcal{L}_{\rm AB}$ and $\mathcal{L}$ (see section 3.5.2), whereas $\mathcal{M}$ and $\mathcal{L}$ combine to describe the amount of entanglement harvested from the field to the detectors (see section 3.5.1). We will analyze these two additional terms independently in the next two sections.

3.2.2.1 Calculation of $\mathcal{L}_{\rm AB}^{\hat{\phi}^2}$

In order to particularize $\mathcal{L}_{\rm AB}^{\hat{\phi}^2}$, Eq. (3.14), to 3+1 dimensional space and two detectors with identical Gaussian switching functions and spatial profiles, we set $\nu = {\rm A}$ and $\mu = {\rm B}$ and then substitute explicit expressions in for $W^{\hat{\phi}^2}$, F, and χ, namely $W^{\hat{\phi}^2}$ in 3+1 spacetime dimensions Eq. (3.72), a Gaussian spatial profile Eq. (3.25), and a Gaussian switching function Eq. (3.26). As is now tradition, we will do the same change of coordinates as in the calculation of the linear VEP, shown in Eq. (3.27). This transformation results in

$$\begin{aligned}\mathcal{L}_{\rm AB}{}^{\hat{\phi}^2} =& \frac{\lambda^2 e^{-\frac{t_{\rm A}^2+t_{\rm B}^2}{T^2}-\frac{\boldsymbol{x}_{\rm A}^2+\boldsymbol{x}_{\rm B}^2}{\sigma^2}}}{128\pi^7\sigma^6}\int_{-\infty}^{\infty}{\rm d}u\, e^{\frac{(t_{\rm A}+t_{\rm B})u}{T^2}-\frac{u^2}{2T^2}}\int {\rm d}^3\boldsymbol{p}\, e^{\frac{\boldsymbol{p}(\boldsymbol{x}_{\rm A}+\boldsymbol{x}_{\rm B})}{\sigma^2}-\frac{\boldsymbol{p}^2}{2\sigma^2}}\\ &\times\int_{-\infty}^{\infty}{\rm d}v\int {\rm d}^3\boldsymbol{q}\,\frac{e^{\frac{\boldsymbol{q}(\boldsymbol{x}_{\rm A}-\boldsymbol{x}_{\rm B})}{\sigma^2}+\frac{v(t_{\rm A}-t_{\rm B})}{T^2}-\frac{\boldsymbol{q}^2}{2\sigma^2}-\frac{v^2}{2T^2}-{\rm i}v\Omega}}{\left(\boldsymbol{q}^2-(v-{\rm i}\epsilon)^2\right)^2}.\end{aligned} \tag{3.82}$$

The integrals over u, $\boldsymbol{p}$, the angular part of $\boldsymbol{q}$, and v can be evaluated in closed form (details are analogous to the calculations in section 3.2.1). Following [36], we rewrite these integrals in terms of the dimensionless quantities outlined in Table 3.1 on page 14. The result is

$$\begin{aligned}\mathcal{L}_{\rm AB}{}^{\hat{\phi}^2} =& \frac{\lambda^2 e^{\alpha\eta-\frac{(\beta)^2}{2\delta^2}-\frac{1}{2}(\gamma_{\rm A}-\gamma_{\rm B})^2+{\rm i}\gamma_{\rm A}\eta-{\rm i}\gamma_{\rm B}\eta+\frac{\eta^2}{2}}}{32\pi^4\delta T^2(\beta)}\int_0^{\infty}{\rm d}\xi\,\frac{e^{-{\rm i}\alpha\xi+\gamma_{\rm A}\xi-\gamma_{\rm B}\xi-\frac{\xi^2}{2\delta^2}-{\rm i}\eta\xi-\frac{\xi^2}{2}}}{\xi^2}\\ &\times\sinh\left(\frac{\xi(\beta)}{\delta^2}\right)\Bigg[\pi\left({\rm i}\alpha\xi-\gamma_{\rm A}\xi+\gamma_{\rm B}\xi+{\rm i}\eta\xi+\xi^2+1\right){\rm erfi}\left(\frac{{\rm i}\alpha-\gamma_{\rm A}+\gamma_{\rm B}+{\rm i}\eta+\xi}{\sqrt{2}}\right)\\ &-2\sqrt{2\pi}\xi e^{-\frac{1}{2}(\alpha+{\rm i}\gamma_{\rm A}-{\rm i}(\gamma_{\rm B}+{\rm i}\eta+\xi))^2}+\pi\Bigg[\alpha\xi+{\rm i}\gamma_{\rm A}\xi-{\rm i}\gamma_{\rm B}\xi+\eta\xi-{\rm i}\xi^2-{\rm i}\\ &+e^{2\xi({\rm i}\alpha-\gamma_{\rm A}+\gamma_{\rm B}+{\rm i}\eta)}\left(\xi\left(\gamma_{\rm A}-\gamma_{\rm B}-{\rm i}\alpha-{\rm i}\eta+\xi\right)+1\right){\rm i}\,{\rm erfc}\left({\rm i}\frac{-{\rm i}\alpha+\gamma_{\rm A}-\gamma_{\rm B}-{\rm i}\eta+\xi}{\sqrt{2}}\right)\Bigg]\Bigg],\end{aligned} \tag{3.83}$$

where ξ is a dummy variable of integration. Taking the limit $\eta \to 0$ of $\mathcal{L}_{\rm AB}{}^{\hat{\phi}^2}$ yields

$$\lim_{\eta\to 0}\mathcal{L}_{\rm AB}{}^{\hat{\phi}^2} = \frac{\lambda^2 e^{-\frac{\beta^2}{2\delta^2}-\frac{1}{2}(\gamma_{\rm A}-\gamma_{\rm B})^2}}{32\pi^3\delta T^2(\beta)}\int_0^\infty \mathrm{d}\xi\,\frac{e^{-\mathrm{i}\alpha\xi+\gamma_{\rm A}\xi-\gamma_{\rm B}\xi-\frac{\xi^2}{2\delta^2}-\frac{\xi^2}{2}}}{\xi^2}\sinh\left(\frac{\xi(\beta)}{\delta^2}\right)$$
$$\times\left[(\alpha\xi+\mathrm{i}\xi(\gamma_{\rm A}-\gamma_{\rm B}-\xi)-\mathrm{i})\mathrm{erfc}\left(\frac{\alpha+\mathrm{i}(\gamma_{\rm A}-\gamma_{\rm B}-\xi)}{\sqrt{2}}\right)-\sqrt{\frac{8}{\pi}}\xi e^{-\frac{1}{2}(\alpha+\mathrm{i}(\gamma_{\rm A}-\gamma_{\rm B}-\xi))^2}\right.$$
$$\left.+\,e^{2\xi(\mathrm{i}\alpha-\gamma_{\rm A}+\gamma_{\rm B})}(\alpha\xi+\mathrm{i}\xi(\gamma_{\rm A}-\gamma_{\rm B}+\xi)+\mathrm{i})\mathrm{erfc}\left(\frac{\alpha+\mathrm{i}(\gamma_{\rm A}-\gamma_{\rm B}+\xi)}{\sqrt{2}}\right)\right], \tag{3.84}$$

which has no divergences. Fig. 3.1 (e) numerically illustrates the behaviour of Eq. (3.84) as the UV cutoff is lifted (as η decreases).

3.2.2.2 Calculation of $\mathcal{M}^{\hat{\phi}^2}$

In the following, we will derive $\mathcal{M}^{\hat{\phi}^2}$. We will see that while $\mathcal{M}^{\hat{\phi}}$ had only regularizable divergences, $\mathcal{M}^{\hat{\phi}^2}$ exhibits persistent UV divergences (i.e., divergences that cannot be regularized with spatial profiles or smooth swithchings, see section 2.4.0.1 for discussion of persistent versus regularizable divergences in UDW detectors). This leads to the soft UV cutoff interpretation of ϵ (see section 3.1.0.1), which is necessary to tame the divergence analyzed in section 3.4.

For the quadratic model, $\mathcal{M}^{\hat{\phi}^2}$ is given by Eq. (3.13). To particularize to 3+1 dimensions and detectors quadratically to the field with identical Gaussian switching functions and spatial smearing, we need to make several substitutions. Namely, we substitute the quadratic two-point correlator in 3+1 dimensions Eq. (3.72), the spatial profile Eq. (3.25), and the switching function Eq. (3.26). The result of all these substitutions plus the change of coordinates (3.27) is

$$\mathcal{M}^{\hat{\phi}^2} = \frac{-\lambda^2 e^{-\frac{t_{\rm A}^2}{T^2}-\frac{t_{\rm B}^2}{T^2}-\frac{\boldsymbol{x}_{\rm A}^2}{\sigma^2}-\frac{\boldsymbol{x}_{\rm B}^2}{\sigma^2}}}{128\pi^5\sigma^6}\int_{-\infty}^{\infty}\mathrm{d}u\,e^{\frac{t_{\rm A}u}{T^2}+\frac{t_{\rm B}u}{T^2}-\frac{u^2}{2T^2}+\mathrm{i}u\Omega}\int\mathrm{d}^3\boldsymbol{p}\,e^{-\frac{p^2}{2\sigma^2}+\frac{q\boldsymbol{x}_{\rm A}}{\sigma^2}+\frac{q\boldsymbol{x}_{\rm B}}{\sigma^2}} \tag{3.85}$$
$$\times\int_{-\infty}^{\infty}\mathrm{d}v\int\mathrm{d}^3\boldsymbol{q}\,\frac{e^{-\frac{v^2}{2T^2}}e^{-\frac{q^2}{2\sigma^2}}}{\left(q^2-(v-\mathrm{i}\epsilon)^2\right)^2}\left[e^{-\frac{q\boldsymbol{x}_{\rm A}}{\sigma^2}+\frac{q\boldsymbol{x}_{\rm B}}{\sigma^2}-\frac{t_{\rm A}v}{T^2}+\frac{t_{\rm B}v}{T^2}}+e^{-(-\frac{q\boldsymbol{x}_{\rm A}}{\sigma^2}+\frac{q\boldsymbol{x}_{\rm B}}{\sigma^2}-\frac{t_{\rm A}v}{T^2}+\frac{t_{\rm B}v}{T^2})}\right].$$

The integrals over u, $\boldsymbol{p}$, and the angular part of $\boldsymbol{q}$ can be evaluated in closed form:

$$\mathcal{M}_{t_{\rm A}=t_{\rm B}}{}^{\hat{\phi}^2} = -\frac{\lambda^2 T e^{-\frac{T^2\Omega^2}{2}+2\mathrm{i}t_{\rm A}\Omega-\frac{(\boldsymbol{x}_{\rm A}-\boldsymbol{x}_{\rm B})^2}{2\sigma^2}}}{4\pi^4\sigma(\boldsymbol{x}_{\rm A}-\boldsymbol{x}_{\rm B})}\int_0^\infty\mathrm{d}q\int_{-\infty}^{\infty}\mathrm{d}v\,\frac{q\sinh\left(\frac{q\,(\boldsymbol{x}_{\rm A}-\boldsymbol{x}_{\rm B})}{\sigma^2}\right)}{\left(q^2-(v-\mathrm{i}\epsilon)^2\right)^2}e^{-\frac{q^2}{2\sigma^2}-\frac{v^2}{2T^2}}. \tag{3.86}$$

Furthermore, we can employ the simplifying assumption that the two detectors are switched on simultaneously within their co-moving frame, setting $t_{\rm A}-t_{\rm B}=0$. The result we write as

$$\mathcal{M}^{\hat{\phi}^2}{}_{t_{\rm A}=t_{\rm B}} = -\frac{\lambda^2 e^{-\frac{\alpha^2}{2}+2\mathrm{i}\alpha\gamma_{\rm A}-\frac{\beta^2}{2\delta^2}}}{64\pi^4\delta T^3\beta}\int_0^\infty\mathrm{d}\xi\,\mathrm{G}\,(\xi)\,, \tag{3.87}$$

where ξ is a dummy integration variable. The full expression of the integrand $G(\xi)$ is defined as

$$\begin{aligned}
\mathrm{G}\left(\xi\right) \coloneqq \frac{1}{\xi^2\left(\eta^2+\xi^2\right)}\sinh\left(\frac{\xi\beta}{\delta^2}\right)e^{-\frac{\xi^2}{2\delta^2}}\Bigg[& -4\xi\left(\sqrt{2\pi}\eta^2-2\mathrm{i}\eta+\sqrt{2\pi}\xi^2\right) \\
& + e^{-\frac{\xi^2}{2}}\left(\eta^2+\xi^2\right)\Bigg(2\mathrm{i}e^{\frac{1}{2}\eta(\eta+2\mathrm{i}\xi)}\Big(\eta\xi+\mathrm{i}\left(\xi^2+1\right)\Big)\Bigg[\mathrm{Chi}\left(\frac{1}{2}(\eta+\mathrm{i}\xi)^2\right) \\
& \quad + \mathrm{i}\pi\mathrm{erf}\left(\frac{\eta+\mathrm{i}\xi}{\sqrt{2}}\right)+2\log(\xi-\mathrm{i}\eta)-\log\left((\eta+\mathrm{i}\xi)^2\right)-\mathrm{Shi}\left(\frac{1}{2}(\eta+\mathrm{i}\xi)^2\right)\Bigg] \\
& \quad + e^{\frac{1}{2}\eta(\eta-2\mathrm{i}\xi)}\Bigg[2\left(\mathrm{i}\eta\xi+\xi^2+1\right)\mathrm{Chi}\left(\frac{1}{2}(\eta-\mathrm{i}\xi)^2\right)+\log\Big(-(\eta-\mathrm{i}\xi)^2\Big) \\
& \quad\quad + 2\pi\left(-\eta\xi+\mathrm{i}\left(\xi^2+1\right)\right)\mathrm{erf}\left(\frac{\eta-\mathrm{i}\xi}{\sqrt{2}}\right)+4\left(\mathrm{i}\eta\xi+\xi^2+1\right)\log(-\xi-\mathrm{i}\eta) \\
& \quad\quad - 2\mathrm{i}\xi(\eta-\mathrm{i}\xi)\log\left((\eta-\mathrm{i}\xi)^2\right)+2\left(-\mathrm{i}\eta\xi-\xi^2-1\right)\mathrm{Shi}\left(\frac{1}{2}(\eta-\mathrm{i}\xi)^2\right) \\
& \quad\quad - 2\Big[\log(\xi+\mathrm{i}\eta)+\log\left((\eta-\mathrm{i}\xi)^2\right)\Big]\Bigg]\Bigg)\Bigg].
\end{aligned} \tag{3.88}$$

Chi and Shi are the cosine and sine hyperbolic integral functions defined as

$$\mathrm{Shi}(z) \coloneqq \int_0^z \mathrm{d}t\,\frac{\sinh(t)}{t} \tag{3.89}$$

$$\mathrm{Chi}(z) \coloneqq \widetilde{\gamma}+\ln z+\int_0^z \mathrm{d}t\,\frac{t\cosh(t)-1}{t}. \tag{3.90}$$

$\widetilde{\gamma}$ is the Euler-Mascheroni constant, and everything is expressed in terms of dimensionless variables as detailed in Table 3.1 on page 14.

3.3 The Unruh-DeWitt detector coupled to a complex field

In previous sections we have limited ourselves to real scalar fields. In this section we will consider a complex scalar field. A complex scalar field can be written in terms of a plane wave expansion in a way analogous to the real-field expansion, Eq. (3.18):

$$\hat{\Phi}(\boldsymbol{x},t)=\int\frac{\mathrm{d}^n\boldsymbol{k}e^{-\epsilon|\boldsymbol{k}|/2}}{\sqrt{2(2\pi)^n|\boldsymbol{k}|}}\left(\hat{a}_k^\dagger\,e^{\mathrm{i}(|\boldsymbol{k}|t-\boldsymbol{k}\cdot\boldsymbol{x})}+\hat{b}_k\,e^{-\mathrm{i}(|\boldsymbol{k}|t-\boldsymbol{k}\cdot\boldsymbol{x})}\right), \tag{3.91}$$

where, $\hat{a}_{\boldsymbol{k}}^\dagger$ $\hat{b}_{\boldsymbol{k}}^\dagger$ (and $\hat{a}_{\boldsymbol{k}}$and $\hat{b}_{\boldsymbol{k}}$) are creation (and annihilation) operators for particles and antiparticles, respectively. These operators satisfy the canonical commutation relations $[\hat{a}_{\boldsymbol{k}_1},\hat{a}_{\boldsymbol{k}_2}^\dagger]=\delta^{(n)}(\boldsymbol{k}_1-\boldsymbol{k}_2)$, $[\hat{b}_{\boldsymbol{k}_1},\hat{b}_{\boldsymbol{k}_2}^\dagger]=\delta^{(n)}(\boldsymbol{k}_1-\boldsymbol{k}_2)$ and $[\hat{a}_{\boldsymbol{k}_1},\hat{b}_{\boldsymbol{k}_2}^\dagger]=0$.

An UDW detector coupled to a charged scalar field must (as is the case with the fermionic detector) couple quadratically, else the Hamiltonian would either be non-self adjoint or would break U(1) symmetry (see [40] for more details). Thus, we use the following Hamiltonian

$$\hat{H}^{\hat{\Phi}\hat{\Phi}^\dagger}(t) = \sum_{\nu\in\{A,B\}} \lambda_\nu \chi_\nu(t-t_\nu)\hat{\mu}_\nu(t) \int \mathrm{d}^n\boldsymbol{x}\, F_\nu(\boldsymbol{x}-\boldsymbol{x}_\nu) : \hat{\Phi}(\boldsymbol{x},t)\hat{\Phi}^\dagger(\boldsymbol{x},t) :, \tag{3.92}$$

where $\nu \in \{\mathrm{A},\mathrm{B}\}$ identifies either detector A or B. As with the real quadratic case, the coupling constant λ does not have the same dimensions the linear coupling constant.

We will follow the process outlined in sections 3.1 (for the linear detector model) and 3.2 (for the quadratic detector model). We find that the time evolved bipartite state of two initially uncorrelated detectors in their ground state,

$$\hat{\rho}_{\mathrm{AB},0} = |g_\mathrm{A}\rangle\langle g_\mathrm{A}| \otimes |g_\mathrm{B}\rangle\langle g_\mathrm{B}|\,, \tag{3.93}$$

which interact through a the vacuum state of a complex field takes the same form as with the linear and quadratic real detectors (as originally shown in Eq. (3.12))

$$\hat{\rho}_{\mathrm{AB,T}} = \begin{pmatrix} 1-\mathcal{L}_{\mathrm{AA}}-\mathcal{L}_{\mathrm{BB}} & 0 & 0 & \mathcal{M}^* \\ 0 & \mathcal{L}_{\mathrm{AA}} & \mathcal{L}_{\mathrm{AB}} & 0 \\ 0 & \mathcal{L}_{\mathrm{BA}} & \mathcal{L}_{\mathrm{BB}} & 0 \\ \mathcal{M} & 0 & 0 & 0 \end{pmatrix} + \mathcal{O}(\lambda_\nu^4),$$

where $\mathcal{M}$ and $\mathcal{L}_{\mu\nu}$ take the form

$$\mathcal{M}^{\hat{\Phi}\hat{\Phi}^\dagger} = -\lambda_\mathrm{A}\lambda_\mathrm{B} \int_{-\infty}^{\infty}\mathrm{d}t \int_{-\infty}^{t}\mathrm{d}t' \int \mathrm{d}^n\boldsymbol{x} \int \mathrm{d}^n\boldsymbol{x}'\, M(t,\boldsymbol{x},t',\boldsymbol{x}')\, W^{\hat{\Phi}\hat{\Phi}^\dagger}(t,\boldsymbol{x},t',\boldsymbol{x}') \tag{3.94}$$

$$\mathcal{L}_{\nu\mu}^{\hat{\Phi}\hat{\Phi}^\dagger} = \lambda_\nu\lambda_\mu \int_{-\infty}^{\infty}\mathrm{d}t \int_{-\infty}^{\infty}\mathrm{d}t' \int \mathrm{d}^n\boldsymbol{x} \int \mathrm{d}^n\boldsymbol{x}'\, L_\nu^*(t,\boldsymbol{x})\, L_\mu(t',\boldsymbol{x}')\, W^{\hat{\Phi}\hat{\Phi}^\dagger}(t,\boldsymbol{x},t',\boldsymbol{x}'), \tag{3.95}$$

where the superscript $\hat{\Phi}\hat{\Phi}^\dagger$ denotes quadratic coupling to the charged scalar field.

As with the previous detectors studied, the effects of the field and coupling is entirely captured by the correlation function W. The functions M and L_ν are defined exactly as Eqs. Eq. (3.16) and Eq. (3.15), namely

$$\begin{aligned} L_\nu(t,\boldsymbol{x}) &= \chi_\nu(t-t_\nu)\, F_\nu(\boldsymbol{x}-\boldsymbol{x}_\nu)\, e^{\mathrm{i}\Omega_\nu t} \\ M(t,\boldsymbol{x},t',\boldsymbol{x}') &= L_\mathrm{A}(t,\boldsymbol{x})L_\mathrm{B}(t',\boldsymbol{x}') + L_\mathrm{A}(t',\boldsymbol{x}')L_\mathrm{B}(t,\boldsymbol{x}). \end{aligned}$$

Utilizing a similar process as was used to arrive at the two-point function Eq. (3.70), we will show that the quadratic detector model's response to a charged (complex) scalar field is within a constant factor to that of a real scalar field.

For the UDW detector coupled to a complex field, $W^{\hat{\Phi}\hat{\Phi}^\dagger}(t,\boldsymbol{x},t',\boldsymbol{x}')$ is

$$W^{\hat{\Phi}\hat{\Phi}^\dagger}(t,\boldsymbol{x},t',\boldsymbol{x}') = \langle 0| : \hat{\Phi}(\boldsymbol{x},t)\hat{\Phi}^\dagger(\boldsymbol{x},t) :: \hat{\Phi}(\boldsymbol{x}',t')\hat{\Phi}^\dagger(\boldsymbol{x}',t') : |0\rangle\,. \tag{3.96}$$

The relationship between an operator $\hat{A}$ and its normal ordered version is given by Eq. (3.57), namely

$$:\hat{A}:=\hat{A}-\langle 0|\,\hat{A}\,|0\rangle$$

Using this identity, $W^{\hat{\Phi}\hat{\Phi}^\dagger}$ can be rewritten as

$$\begin{aligned}W^{\hat{\Phi}\hat{\Phi}^\dagger}(t,\boldsymbol{x},t',\boldsymbol{x}')=&\langle 0|\,\hat{\Phi}(\boldsymbol{x},t)\hat{\Phi}^\dagger(\boldsymbol{x},t)\hat{\Phi}(\boldsymbol{x}',t')\hat{\Phi}^\dagger(\boldsymbol{x}',t')\,|0\rangle\\&-\langle 0|\,\hat{\Phi}(\boldsymbol{x},t)\hat{\Phi}^\dagger(\boldsymbol{x},t)\,|0\rangle\,\langle 0|\,\hat{\Phi}(\boldsymbol{x}',t')\hat{\Phi}^\dagger(\boldsymbol{x}',t')\,|0\rangle\,.\end{aligned}\tag{3.97}$$

The first term of $W^{\hat{\Phi}\hat{\Phi}^\dagger}(t,\boldsymbol{x},t',\boldsymbol{x}')$ can be simplified. To do so, we will write the field operator as $\hat{\Phi}=\hat{\Phi}^+ + \hat{\Phi}^-$, where $\hat{\Phi}^+$ and $\hat{\Phi}^-$ are defined as

$$\hat{\Phi}^+(\boldsymbol{x},t)=\int\frac{\mathrm{d}^n\boldsymbol{k}\,e^{-\epsilon|\boldsymbol{k}|/2}}{\sqrt{2(2\pi)^n|\boldsymbol{k}|}}\,\hat{a}_k^\dagger\,e^{\mathrm{i}(|\boldsymbol{k}|t-\boldsymbol{k}\cdot\boldsymbol{x})},\qquad\hat{\Phi}^-(\boldsymbol{x},t)=\int\frac{\mathrm{d}^n\boldsymbol{k}\,e^{-\epsilon|\boldsymbol{k}|/2}}{\sqrt{2(2\pi)^n|\boldsymbol{k}|}}\,\hat{b}_k\,e^{-\mathrm{i}(|\boldsymbol{k}|t-\boldsymbol{k}\cdot\boldsymbol{x})},\tag{3.98}$$

where the operators $\hat{\Phi}^+$ and $\hat{\Phi}^-$ satisfy the commutation relation

$$\left[\hat{\Phi}^-(\boldsymbol{x}_\mu,t_\mu),\hat{\Phi}^+(\boldsymbol{x}_\nu,t_\nu)\right]=0,\tag{3.99}$$

and

$$\left[\hat{\Phi}^-(\boldsymbol{x}_\mu,t_\mu),\hat{\Phi}^{-\dagger}(\boldsymbol{x}_\nu,t_\nu)\right]=\mathcal{C}_{\mu\nu}\mathbb{1},\qquad\left[\hat{\Phi}^+(\boldsymbol{x}_\mu,t_\mu),\hat{\Phi}^{+\dagger}(\boldsymbol{x}_\nu,t_\nu)\right]=\mathcal{C}_{\nu\mu}\mathbb{1},\tag{3.100}$$

where $\mathcal{C}_{\mu\nu}\in\mathbb{C}$ is precisely that in Eq. (3.60), namely,

$$\mathcal{C}_{\mu\nu}=\int\frac{\mathrm{d}^n\boldsymbol{k}\,e^{-\epsilon|\boldsymbol{k}|/2}}{2(2\pi)^n|\boldsymbol{k}|}e^{\mathrm{i}(|\boldsymbol{k}|(t_\nu-t_\mu)-\boldsymbol{k}\cdot(\boldsymbol{x}_\nu-\boldsymbol{x}_\mu))}$$

Furthermore, if we define $\hat{\Phi}_\nu$ such that

$$\langle 0|\,\hat{\Phi}(\boldsymbol{x},t)\hat{\Phi}^\dagger(\boldsymbol{x},t)\hat{\Phi}(\boldsymbol{x}',t')\hat{\Phi}^\dagger(\boldsymbol{x}',t')\,|0\rangle=\langle 0|\,\hat{\Phi}_1\hat{\Phi}_2^\dagger\hat{\Phi}_3\hat{\Phi}_4^\dagger\,|0\rangle\,,\tag{3.101}$$

we can use $\hat{\Phi}^+$ and $\hat{\Phi}^-$ (and their adjoints) to rewrite the first term in Eq. (3.97) as

$$\langle 0|\hat{\Phi}_1\hat{\Phi}_2^\dagger\hat{\Phi}_3\hat{\Phi}_4^\dagger\,|0\rangle=\langle 0|\,\hat{\Phi}_1^-\hat{\Phi}_2^{-\dagger}\hat{\Phi}_3^-\hat{\Phi}_4^{-\dagger}\,|0\rangle+\langle 0|\,\hat{\Phi}_1^-\hat{\Phi}_2^{+\dagger}\hat{\Phi}_3^-\hat{\Phi}_4^{+\dagger}\,|0\rangle\,.\tag{3.102}$$

Note that here the expression differs from the real case (see Eq. (3.62)), although we still use that

$$\hat{\phi}_\mu^{+\dagger}\,|0\rangle=\langle 0|\,\hat{\phi}_\nu^+=\hat{\phi}_\mu^-\,|0\rangle=\langle 0|\,\hat{\phi}_\nu^{-\dagger}=0\tag{3.103}$$

and that only summands with as many $\hat{\Phi}^-$ as $\hat{\Phi}^{-\dagger}$ and $\hat{\Phi}^+$ as $\hat{\Phi}^{+\dagger}$ give a non-vanishing vacuum expectation

By commuting operators using Eq. (3.60), we can write the the following

$$\langle 0|\,\hat{\Phi}_1^-\hat{\Phi}_2^{-\dagger}\hat{\Phi}_3^-\hat{\Phi}_4^{-\dagger}\,|0\rangle = \mathcal{C}_{23}\mathcal{C}_{14}\,\langle 0|\,\hat{\Phi}_1^-\hat{\Phi}_2^+\hat{\Phi}_3^-\hat{\Phi}_4^+\,|0\rangle = \mathcal{C}_{12}\mathcal{C}_{34}. \tag{3.104}$$

Thus Eq. (3.102) can be written as

$$\langle 0|\hat{\Phi}_1\hat{\Phi}_2\hat{\Phi}_3\hat{\Phi}_4\,|0\rangle = \mathcal{C}_{23}\mathcal{C}_{14} + \mathcal{C}_{12}\mathcal{C}_{34}. \tag{3.105}$$

We can rewrite the $\mathcal{C}_{\mu\nu}$ coefficients as

$$\mathcal{C}_{\mu\nu} = \langle 0|\left[\hat{\Phi}_\mu^-, \hat{\Phi}_\nu^{-\dagger}\right]|0\rangle = \langle 0|\,\hat{\Phi}_\mu^-\hat{\Phi}_\nu^{-\dagger}\,|0\rangle = \langle 0|\,\hat{\Phi}_\mu\hat{\Phi}_\nu^\dagger\,|0\rangle\,, \tag{3.106}$$

which allows us to rewrite Eq. (3.65) as

$$\langle 0|\hat{\Phi}_1\hat{\Phi}_2\hat{\Phi}_3\hat{\Phi}_4\,|0\rangle = \langle 0|\,\hat{\Phi}_1\hat{\Phi}_2^\dagger\,|0\rangle\,\langle 0|\,\hat{\Phi}_3\hat{\Phi}_4^\dagger\,|0\rangle + \langle 0|\,\hat{\Phi}_1\hat{\Phi}_3^\dagger\,|0\rangle\,\langle 0|\,\hat{\Phi}_2\hat{\Phi}_4^\dagger\,|0\rangle\,. \tag{3.107}$$

Using our definition of $\hat{\Phi}_\nu$ in Eq. (3.101), this becomes

$$\begin{aligned}\langle 0|\,\hat{\Phi}(\boldsymbol{x},t)\hat{\Phi}^\dagger(\boldsymbol{x},t)\hat{\Phi}(t',\boldsymbol{x}')\hat{\Phi}^\dagger(t',\boldsymbol{x}')\,|0\rangle &= \langle 0|\,\hat{\Phi}(\boldsymbol{x},t)\hat{\Phi}^\dagger(\boldsymbol{x},t)\,|0\rangle\,\langle 0|\,\hat{\Phi}(t',\boldsymbol{x}')\hat{\Phi}^\dagger(t',\boldsymbol{x}')\,|0\rangle \\ &\quad + \langle 0|\,\hat{\Phi}(\boldsymbol{x},t)\hat{\Phi}^\dagger(t',\boldsymbol{x}')\,|0\rangle\,\langle 0|\,\hat{\Phi}(\boldsymbol{x},t)\hat{\Phi}^\dagger(t',\boldsymbol{x}')\,|0\rangle\,.\end{aligned} \tag{3.108}$$

Thus the complex correlation function, originally expressed in Eq. (3.97), is

$$W^{\phi\phi^\dagger}(t,\boldsymbol{x},t',\boldsymbol{x}') = \Big(\langle 0|\,\hat{\Phi}(\boldsymbol{x},t)\hat{\Phi}^\dagger(\boldsymbol{x}',t')\,|0\rangle\Big)^2. \tag{3.109}$$

At this point, we will now make a comparison of Eq. (3.109) with the correlation function of the real quadratic normal ordered field operator, Eq. (3.69):

$$W^{\hat{\phi}^2}(t,\boldsymbol{x},t',\boldsymbol{x}') = 2\left(\langle 0|\,\hat{\phi}(t,\boldsymbol{x})\hat{\phi}(t',\boldsymbol{x}')\,|0\rangle\right)^2,$$

Using the mode expansions for the complex field, Eq. (3.91) we can rewrite $\langle 0|\,\hat{\Phi}(t,\boldsymbol{x})\hat{\Phi}^\dagger(t',\boldsymbol{x}')\,|0\rangle$ from Eq. (3.109) as

$$\begin{aligned}\langle 0|\,\hat{\Phi}(t,\boldsymbol{x})\hat{\Phi}(t',\boldsymbol{x}')\,|0\rangle = \langle 0|\,\Bigg[&\int \frac{\mathrm{d}^n\boldsymbol{k}e^{-\epsilon|\boldsymbol{k}|/2}}{\sqrt{2(2\pi)^n|\boldsymbol{k}|}}\left(\hat{a}_k^\dagger\, e^{\mathrm{i}(|\boldsymbol{k}|t-\boldsymbol{k}\cdot\boldsymbol{x})} + \hat{b}_k\, e^{-\mathrm{i}(|\boldsymbol{k}|t-\boldsymbol{k}\cdot\boldsymbol{x})}\right) \\ &\times\int \frac{\mathrm{d}^n\boldsymbol{k}e^{-\epsilon|\boldsymbol{k}|/2}}{\sqrt{2(2\pi)^n|\boldsymbol{k}|}}\left(\hat{a}_k\, e^{-\mathrm{i}(|\boldsymbol{k}|t'-\boldsymbol{k}\cdot\boldsymbol{x}')} + \hat{b}_k^\dagger\, e^{\mathrm{i}(|\boldsymbol{k}|t'-\boldsymbol{k}\cdot\boldsymbol{x}')}\right)\Bigg]\,|0\rangle\,.\end{aligned} \tag{3.110}$$

which simplifies to

$$\langle 0|\,\hat{\Phi}(t,\boldsymbol{x})\hat{\Phi}(t',\boldsymbol{x}')\,|0\rangle = \int \frac{\mathrm{d}^n\boldsymbol{k}e^{-\epsilon|\boldsymbol{k}|}}{2(2\pi)^n|\boldsymbol{k}|}e^{-\mathrm{i}(|\boldsymbol{k}|t-\boldsymbol{k}\cdot\boldsymbol{x})}e^{\mathrm{i}(|\boldsymbol{k}|t'-\boldsymbol{k}\cdot\boldsymbol{x}')}. \tag{3.111}$$

Using the mode expansions for the real field, Eq. (3.18), we can rewrite the two point correlator of the real field, $\langle 0|\,\hat{\phi}(t,\boldsymbol{x})\hat{\phi}(t',\boldsymbol{x}')\,|0\rangle$, as

$$\begin{aligned}\langle 0|\,\hat{\phi}(t,\boldsymbol{x})\hat{\phi}(t',\boldsymbol{x}')\,|0\rangle = \langle 0|\Bigg[\int \frac{\mathrm{d}^n\boldsymbol{k}e^{-\epsilon|\boldsymbol{k}|/2}}{\sqrt{2(2\pi)^n|\boldsymbol{k}|}}\left(\hat{a}_k^\dagger\, e^{\mathrm{i}(|\boldsymbol{k}|t-\boldsymbol{k}\cdot\boldsymbol{x})}+\hat{a}_k\, e^{-\mathrm{i}(|\boldsymbol{k}|t-\boldsymbol{k}\cdot\boldsymbol{x})}\right)\\ \times\int \frac{\mathrm{d}^n\boldsymbol{k}e^{-\epsilon|\boldsymbol{k}|/2}}{\sqrt{2(2\pi)^n|\boldsymbol{k}|}}\left(\hat{a}_k\, e^{-\mathrm{i}(|\boldsymbol{k}|t'-\boldsymbol{k}\cdot\boldsymbol{x}')}+\hat{a}_k^\dagger\, e^{\mathrm{i}(|\boldsymbol{k}|t'-\boldsymbol{k}\cdot\boldsymbol{x}')}\right)\Bigg]|0\rangle\,.\end{aligned} \tag{3.112}$$

which simplifies to

$$\langle 0|\,\hat{\phi}(t,\boldsymbol{x})\hat{\Phi}(t',\boldsymbol{x}')\,|0\rangle = \int \frac{\mathrm{d}^n\boldsymbol{k}e^{-\epsilon|\boldsymbol{k}|}}{2(2\pi)^n|\boldsymbol{k}|}e^{-\mathrm{i}(|\boldsymbol{k}|t-\boldsymbol{k}\cdot\boldsymbol{x})}e^{\mathrm{i}(|\boldsymbol{k}|t'-\boldsymbol{k}\cdot\boldsymbol{x}')}. \tag{3.113}$$

Thus we find that the relation between the complex and real correlation functions is

$$W^{\phi\phi^\dagger}(t,\boldsymbol{x},t',\boldsymbol{x}') = \frac{1}{2}W^{\hat{\phi}^2}(t,\boldsymbol{x},t',\boldsymbol{x}'). \tag{3.114}$$

As a side note, while the Hamiltonian is self adjoint, there is an asymmetry between the coupling to the particle and antiparticle sectors (pointed out in [40]). The coupling can be symmetrized,

$$H_I \propto \Phi\Phi^\dagger + \Phi^\dagger\Phi \tag{3.115}$$

to avoid this. This symmetrization will give a factor 2, thus making the detector response to charged and real fields exactly the same. This together motivates future studies utilizing the symmetrized coupling.

3.4 Divergences in the quadratic model

In this section we will discuss a new kind of divergence that appears in the quadratic model. This divergence appears for detectors coupled to either real or charged fields, and discussion applies to both, since the the wightman functions are proportional. All expression are particularized to detectors coupled to the real field.

Unlike the linear model, the non-local term $\mathcal{M}^{\hat{\phi}^2}$ is not free of UV divergences, despite the fact that the detector has a smooth switching and a Gaussian spatial smearing, and despite the renormalization process (outlined in [40]) that removed the single-detector divergences. Concretely, the integral in Eq. (3.87) is logarithmically divergent with the UV cutoff scale, as illustrated in Fig. 3.1.(f).

To gain insight on the logarithmic divergence in $\mathcal{M}^{\hat{\phi}^2}$ we examine the integrand $G(\xi)$, defined in equation Eq. (3.88).

We begin by noticing that $G(\xi)$ has the limit $\eta \to 0$

$$\lim_{\eta\to 0} G(\xi) = \frac{4}{\xi^2} e^{-\frac{\left(\delta^2+1\right)\xi^2}{2\delta^2}} \sinh\left(\frac{\xi\beta}{\delta^2}\right)\left[-\sqrt{2\pi}e^{\frac{\xi^2}{2}}\xi + \mathrm{i}\pi\left(\xi^2+1\right)\operatorname{erfc}\left(\frac{\mathrm{i}\xi}{\sqrt{2}}\right)\right]. \quad (3.116)$$

Expanding in Laurent series and keeping the leading order $\mathcal{O}(\xi^{-1})$ results in the UV divergent term

$$\lim_{\eta\to 0} G_{\mathcal{M}^{\hat{\phi}^2}{}_{t_{\mathrm{A}}=t_{\mathrm{B}}}} \sim \frac{4\mathrm{i}\pi\beta}{\delta^2\xi}. \quad (3.117)$$

This divergence is peculiar due to the fact that it shows up only in the two-detector model, in spite of the fact that the VEP for the quadratic detector model is finite as discussed in section 3.2.1 and in [40]. Thus, while a single quadratically coupled detector does not require additional UV regularization, a cutoff is required for certain quantities describing detector pairs, of which the $\mathcal{M}$ term in Eq. (3.87) is an example.

We would like to emphasize that these are *persistent* UV divergences, that is, they are present regardless of the use of smooth switching functions and spatial profiles (for example, in this case we have used Gaussian functions for both). Moreover, these divergences appear after renormalization of the zero-point energy and at the same order in perturbation theory at which the single detector dynamics is regular.

3.5 Harvesting correlations

To tackle the problem of entanglement harvesting with a pair of quadratically coupled detectors, we will follow two different avenues: a) We will analyze the nature and strength of the divergences in 3+1D flat spacetime, analyzing possible physically motivated regularization scales in entanglement harvesting and b) we will propose a measure of correlations between the detectors that are divergence free and use it to further our knowledge of the differences between the use of linear and quadratic couplings of particle detectors to study the entanglement structure of quantum fields.

In this section we will study two types of correlations that the two detector models can harvest from the field vacuum: a) those measured by the mutual information, which quantifies both classical and quantum correlations [82], and b) the entanglement negativity, which is a faithful entanglement measure for bipartite two-level systems [80]. These two types of correlation harvesting were studied for the linear model in [36]. Here we will compare these results with the predictions for the real-field quadratic model. Further more, we can extrapolate from the quadratic results presented here to the the results for detectors coupled to a complex field, as the associated correlation functions are proportional.

3.5.1 Entanglement harvesting

We consider first the harvesting of entanglement from the vacuum and we quantify it with the entanglement negativity Eq. (2.1) acquired between the two (initially uncorrelated) detectors through their interactions with the field while remaining spacelike separated.

As seen, for instance, in [36], the entanglement negativity can be expressed in terms of the vacuum excitation probability, $\mathcal{L}_{\nu\nu}$, of each detector and the non-local term $\mathcal{M}$. Concretely, it is given by

$$\mathcal{N} = \max\left[\mathcal{N}^{(2)}, 0\right] + \mathcal{O}(\lambda^2), \tag{3.118}$$

where

$$\mathcal{N}^{(2)} = -\frac{1}{2}\left(\mathcal{L}_{\text{AA}} + \mathcal{L}_{\text{BB}} - \sqrt{\left(\mathcal{L}_{\text{AA}} - \mathcal{L}_{\text{BB}}\right)^2 + 4\left|\mathcal{M}\right|^2}\right). \tag{3.119}$$

When both detectors are identical (i.e. they have the same spatial profile, switching function, coupling strength, and detector gap), Eq. (3.119) becomes

$$\mathcal{N}^{(2)} = \left|\mathcal{M}\right| - \mathcal{L}_{\nu\nu} \tag{3.120}$$

from which we can justify the usual argument that entanglement emerges as a competition between the non-local contribution $\mathcal{M}$ and the noise associated to the VEP for each detector [35, 36].

Figure 3.3 shows the behavior of the entanglement negativity with the spatial separation of the detectors, for the linear and quadratic case and a range of detector cutoffs.

Recall that the term $\mathcal{M}$ is UV divergent in the quadratic model, therefore to compute a physically meaningful value for the entanglement negativity further regularization and eventual renormalization would be required. However for a fixed UV-cutoff scale, it is possible to get an estimate of the quadratic model performance to harvest entanglement relative to the linear model by computing entanglement harvesting for both models applying the same UV-cutoff scale. What is more, studying how entanglement negativity changes as we start increasing the cutoff scale will help us see how the UV divergence of $\mathcal{M}$ impacts entanglement harvesting.

As seen in Fig. 3.3, the magnitude of entanglement harvesting increases linearly with the logarithm of the cutoff, which is not surprising since the two-detector quadratic model suffers a logarithmic UV divergence. This implies that there would always exist a value for the cutoff scale so that harvesting is possible at any distance, regardless of the detector gap. It would also imply that for large enough cutoff frequencies we could always 'harvest' more entanglement with the quadratic model than for the linear model.

One can therefore ask the following question: is there any finite value of the cutoff scale that we could take in order to give some physical meaning to the finite cutoff results?

Unlike the linear model—which has been shown to capture the fundamental features of the atom-light interaction [66, 71]— the quadratic model does not have a direct comparison with something as simple as the atom-light interaction mechanism (maybe one could think of non-linear optical media [99], but that is perhaps a stretch). Recall, however, that we do not use the quadratic Unruh-DeWitt model to necessarily reproduce the physics of a particular experimentally motivated setup. Our motivation to explore this model is double: a) probe the field with a different model to show model independence/dependence of harvesting phenomena and b) advance towards the fermionic model (which is a quadratic model that does indeed have physical motivation) where the study of field entanglement remains still full of open questions.

The fact that this model cannot be connected with something as simple as an atom interacting with light, makes it difficult to motivate a choice of cutoff. However, if we were to take the result for a finite value of the cutoff scale seriously, and thus if we were to choose some physically motivated cutoff, we could compare the two models when such a cutoff is taken to be the Planck Frequency. In this scenario, the dimensionless cutoff parameter η can be written as $\eta = \frac{1}{k_{\rm P} T}$, where $\mathrm{k_P}$ is the Planck frequency. If we consider scales for the detector gap Ω to be commensurate with the energy of the first transition of Hydrogen $\Omega_{\rm H} \approx 10^{15}\ \mathrm{s}^{-1}$, then $k_{\rm P} = 10^{29}\Omega$. If we set $T \approx \Omega_{\rm H}^{-1}$ (which means that $\alpha \approx 1$ represents the case of a Hydrogen atom) the cutoff associated with the Planck time is then $\eta = 10^{-29}$. We can extrapolate the results in Fig. 3.2 to the Planck scale. We show these results also in Fig 3.2, as the thin black lines. These plots illustrate the slow logarithmic nature of the divergences, which makes the study of entanglement negativity still meaningful for low energies with the quadratic detector model and does not get significantly qualitatively modified even if the cutoff is transplanckian.

3.5.2 Harvesting mutual information

A way around the problems associated to the UV-divergent nature of $\mathcal{M}$ is to look at UV-safe quantities. Namely, it is possible to find quantifiers of correlations that are, by construction, UV-safe for the quadratic model. One such figure of merit is the mutual information.

For a density matrix of the form Eq. (3.12), the mutual information Eq. (2.3) is given by [36]

$$I(\rho_{\rm AB}) = \mathcal{L}_+ \log(\mathcal{L}_+) + \mathcal{L}_- \log(\mathcal{L}_-) - \mathcal{L}_{\rm AA} \log(\mathcal{L}_{\rm AA}) - \mathcal{L}_{\rm BB} \log(\mathcal{L}_{\rm BB}) + \mathcal{O}(\lambda_\nu^4) \tag{3.121}$$

where

$$\mathcal{L}_\pm = \frac{1}{2}\left(\mathcal{L}_{\rm AA} + \mathcal{L}_{\rm BB} \pm \sqrt{(\mathcal{L}_{\rm AA} - \mathcal{L}_{\rm BB})^2 + 4\,|\mathcal{L}_{\rm AB}|^2}\right). \tag{3.122}$$

Note how $I(\rho_{\rm AB})$ is not dependent on the divergent $\mathcal{M}$ term at leading order in perturbation theory. Hence, the mutual information is finite without any further regularization. Because of this, it provides a UV-cutoff independent sense of the harvesting of correlations from the vacuum, and can also be compared with previous results for the linear

detector model in [36], making it a relevant figure of merit for the comparison in this article.

Fig. 3.4 shows the behavior of the Mutual information with spatial and temporal separation of the detectors for both the linear and quadratic case where the other parameters are the same as those used in Fig 3.2. First, we observe something that was already present in previous literature on linear detector models [36]: Unlike entanglement, the mutual information harvesting can be performed at any distance and detector gap, albeit less efficiently as the distance (or the detector gap) increases, a feature that comes from the fact that the detectors are harvesting classical correlations as well as quantum correlations.

From Fig. 3.4 we observe that the linear detector model can harvest more entanglement and for further distances than the quadratic detector model. This can in turn be used to assess the scale at which the soft cutoff model introduced in the study of entanglement negativity fails to capture the behaviour of UV-safe measures of correlations: as illustrated in Fig 3.3, for cutoff scales that are of the order of $\eta \gtrsim 10^{-6}$, the linear model can harvest more entanglement than the quadratic model in the parameter region studied. This might suggest that comparison of entanglement negativity between the two models can be trusted only for cutoffs above $\eta = 10^{-6}$.

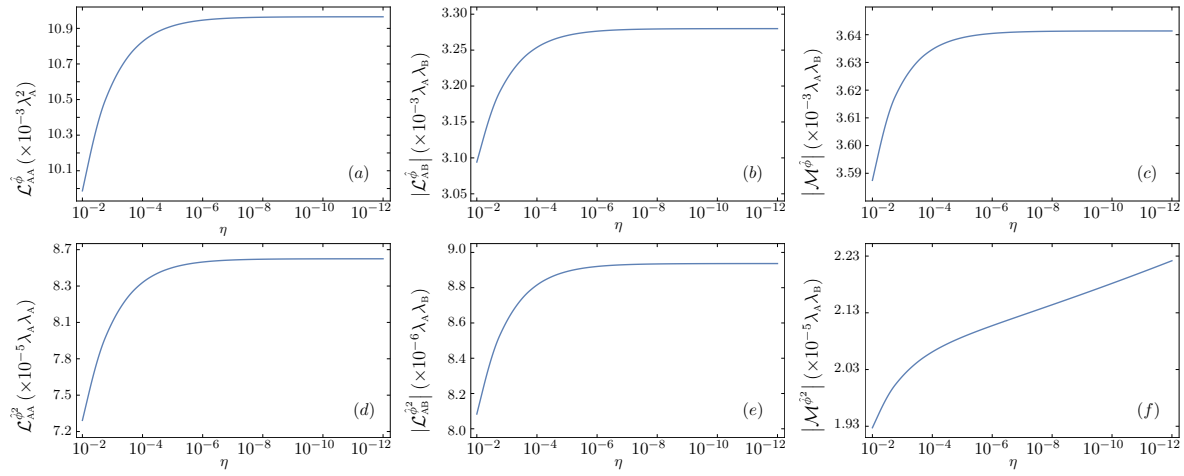

Figure 3.1: All plots illustrate the behavior of relevant quantities as η decreases on a log scale (i.e. as the UV cutoff is lifted). Plots on the top row are for the usual (linearly coupled) UDW detector. Plots on the bottom row are for the quadratically coupled UDW detector. All plots use parameters $\alpha = 1$, $\delta = 1$, $\gamma_{\rm B} - \gamma_{\rm A} = 4$, and $\beta = 4$, where relevant. Note how all plots (a)-(e) indicate convergence, except (f), which (in contrast to (c)) shows shows linear growth of $\mathcal{M}^{\hat{\phi}2}$ on a logarithmic scale of η, and thus a logarithmic divergence as the UV cutoff is lifted, $\eta \to 0$.

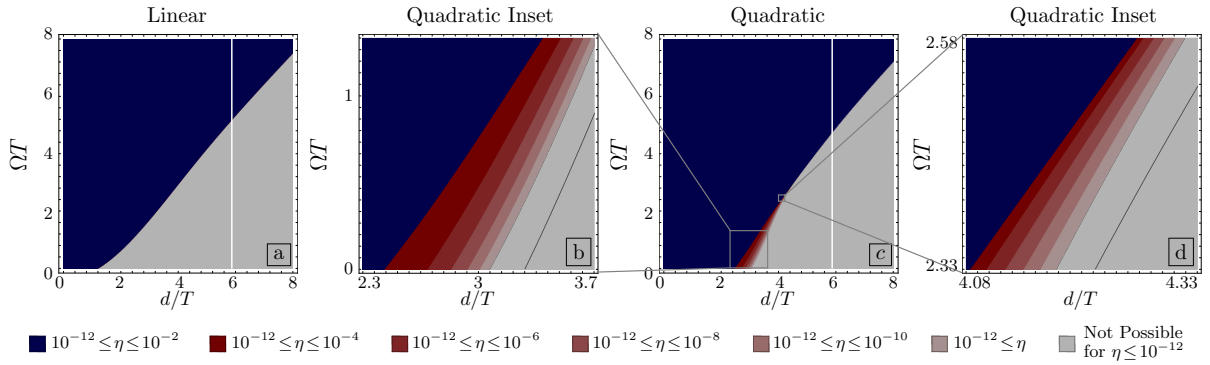

Figure 3.2: Entanglement harvesting is possible (darker regions colored red or blue) for any detector separation d given a sufficiently large detector gap Ω. These plots show various detector cutoffs, $\epsilon = \eta/T$, ranging from $\eta = 10^{-2}$ to $\eta = 10^{-12}$. Note the cutoff does not make a significant difference for the linear model (no visible red regions), while there is a marked increase in the harvesting region for smaller cutoffs (see inset (b) and (c)). Both plots use parameters $\delta = 1$ and $\gamma_{\rm B} - \gamma_{\rm A} = 0$. The vertical white line shows the light cone. The dark lines in the insets are an extrapolation indicating the boundary of where harvesting is no longer possible for a cutoff $\eta = 10^{-29}$ (corresponding to setting the cutoff scale to the Planck frequency, as described at the end of section 3.5.1).

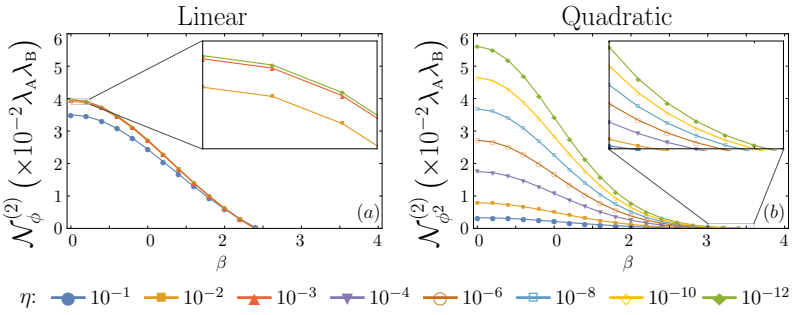

Figure 3.3: The magnitude of entanglement harvested is dependent on the cutoff chosen. For the same cutoff, either the linear or quadratic models may harvest more entanglement, although the linear model quickly converges to a fixed value, while the quadratic model grows logarithmically with decreasing cutoff. Thus, a cutoff can always be chosen sufficiently high such that the quadratic model harvests more entanglement for a given set of parameters. Here, the plots show the leading order contribution to the entanglement negativity with increasing spatial distance. (a) show these results for the linear model while (b) shows these results for the quadratic model. The insets in each plot show where the negativity goes to zero." should read "The inset in (a) shows the convergent behaviour of the negativity, while the inset in (b) shows how the distance at which the negativity goes zero increases as the UV cutoff is lifted. All plots use parameters $\delta = 1$ *and* $\gamma_B\gamma_A = 0$ *and* $\Omega = 1$.

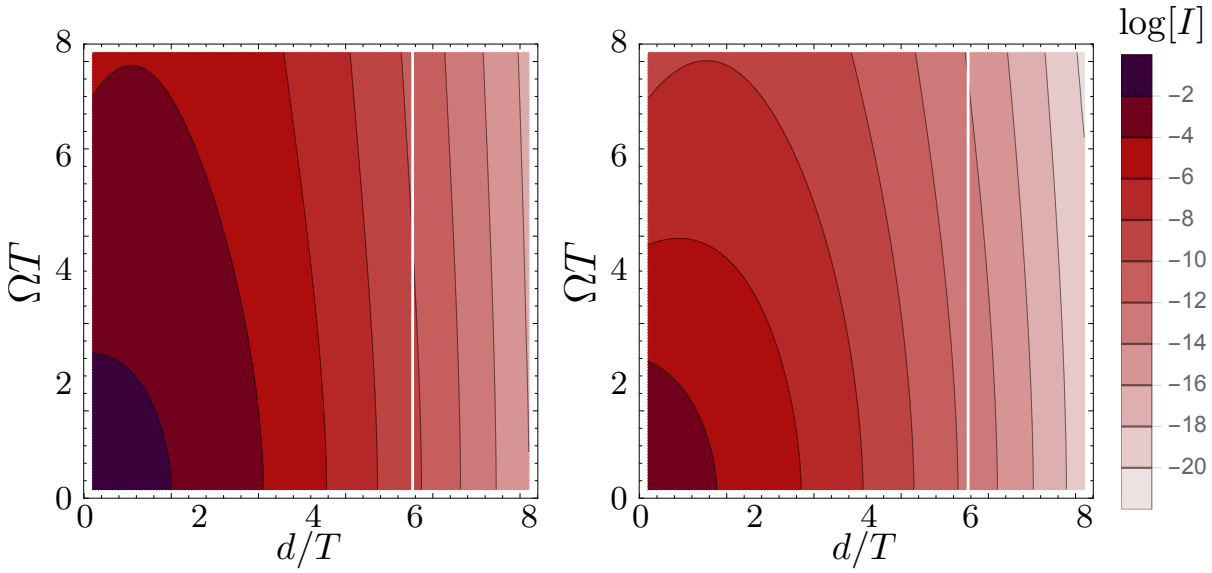

Figure 3.4: Linear mutual information harvesting (left) is greater in magnitude that quadratic mutual entanglement harvesting (right). Legend indicates $\log_{10}(I)$*.Both plots use parameters* $\delta = 1$ *and* $\gamma_B - \gamma_A = 0$*. The thick black line shows the light cone.*

Chapter 4

Conclusion and suggestions for further work

4.1 Conclusion

We have studied the behaviour of pairs of particle detectors quadratically coupled to scalar fields introduced in [37–39] and renormalized in [40]. In particular we have focused on the case of a pair of particle detectors harvesting entanglement from a scalar field, a case previously studied only for linear detectors [34–36]. Understanding the harvesting of correlations from quadratic couplings is a crucial step in understanding the entanglement of Fermionic fields, since detectors must probe these fields with a quadratic coupling [37, 38, 40, 100]. Our motivation to explore this model is twofold: a) probe the field with a different particle detector model to show model independence/dependence of harvesting phenomena and b) provide a model that can be compared on equal footing for bosonic and fermionic fields (for which the coupling necessarily has to be quadratic).

Perhaps the most remarkable finding of our investigation of harvesting with the quadratic detector model is the appearance of a new logarithmic UV divergence at leading order in the two-detector setup. Notably, this divergence remains even when the Hamiltonian is normal-ordered, and even when the switching functions and spatial profile are smooth functions. This is in stark contrast with the linear case where smooth smearing [94] or switching [93, 95] were enough to guarantee the UV regularity of the model.

We emphasize that a single detector, at the same order in perturbation theory, does not present this kind of divergence. Curiously, the UV divergence is only present in a particular kind of term, namely that responsible for the entanglement of the two detectors. This divergence is easily parametrized via a UV cutoff.

Once this was established, analysis and comparison with the linear model was possible. We proceeded in two different ways. First, by using entanglement negativity to study

entanglement harvesting. We discussed whether a finite value of the UV cutoff scale allows for fair comparison of the entanglement harvesting ability of the quadratic and the linear couplings. Following this, we found measures of harvested correlations that are UV-safe. In particular we showed that the harvested mutual information from the field vacuum is UV safe. It therefore constitutes a better figure of merit to compare the harvesting of correlations from the vacuum without need for further regularization.

4.2 Fermionic entanglement harvesting

Understanding the particulars of entanglement harvesting with bosonic quadratic coupling is important in order to properly answer questions about fermionic fields where the study of field entanglement remains full of open questions [2–19]. A comparison of bosonic and fermionic entanglement harvesting on equal footing requires knowledge of the model-dependence entanglement harvesting, specifically the difference between linear and quadratic coupling, as the latter is necessarily present in the fermionic case. The entanglement structure of the fermionic vacuum remains an interesting open question, one we are now prepared to address using the results we have obtained.

Lastly, this thesis posits the question: how can this particular model be renormalized for future studies of entanglement harvesting with the fermionic UDW detector model.

Bibliography

[1] A. Sachs, R. Mann, and E. Martín-Martínez, *Entanglement harvesting and divergences in quadratic Unruh-DeWitt detectors pairs.* To appear in Phys. Rev. D - arXiv:1704.08263, 2017.

[2] M. Montero and E. Martín-Martínez, "Fermionic entanglement ambiguity in noninertial frames," *Phys. Rev. A*, vol. 83, p. 062323, Jun 2011.

[3] K. Brádler and R. Jáuregui, "Comment on "fermionic entanglement ambiguity in noninertial frames"," *Phys. Rev. A*, vol. 85, p. 016301, Jan 2012.

[4] M. Montero and E. Martín-Martínez, "Reply to "comment on 'fermionic entanglement ambiguity in noninertial frames' "," *Phys. Rev. A*, vol. 85, p. 016302, Jan 2012.

[5] P. M. Alsing, I. Fuentes-Schuller, R. B. Mann, and T. E. Tessier, "Entanglement of dirac fields in noninertial frames," *Phys. Rev. A*, vol. 74, p. 032326, Sep 2006.

[6] E. Martín-Martínez and J. León, "Fermionic entanglement that survives a black hole," *Phys. Rev. A*, vol. 80, p. 042318, Oct 2009.

[7] E. Martín-Martínez and J. León, "Quantum correlations through event horizons: Fermionic versus bosonic entanglement," *Phys. Rev. A*, vol. 81, p. 032320, Mar 2010.

[8] E. Martín-Martínez and J. León, "Population bound effects on bosonic correlations in noninertial frames," *Phys. Rev. A*, vol. 81, p. 052305, May 2010.

[9] I. Fuentes, R. B. Mann, E. Martín-Martínez, and S. Moradi, "Entanglement of dirac fields in an expanding spacetime," *Phys. Rev. D*, vol. 82, p. 045030, Aug 2010.

[10] D. E. Bruschi, J. Louko, E. Martín-Martínez, A. Dragan, and I. Fuentes, "Unruh effect in quantum information beyond the single-mode approximation," *Phys. Rev. A*, vol. 82, p. 042332, Oct 2010.

[11] E. Martín-Martínez, L. J. Garay, and J. León, "Unveiling quantum entanglement degradation near a schwarzschild black hole," *Phys. Rev. D*, vol. 82, p. 064006, Sep 2010.

[12] E. Martín-Martínez and I. Fuentes, "Redistribution of particle and antiparticle entanglement in noninertial frames," *Phys. Rev. A*, vol. 83, p. 052306, May 2011.

[13] M. Montero and E. Martín-Martínez, "Entanglement of arbitrary spin fields in noninertial frames," *Phys. Rev. A*, vol. 84, p. 012337, Jul 2011.

[14] M. Montero and E. Martín-Martínez, "The entangling side of the unruh-hawking effect," *Journal of High Energy Physics*, vol. 2011, no. 7, p. 6, 2011.

[15] M. Montero, J. León, and E. Martín-Martínez, "Fermionic entanglement extinction in noninertial frames," *Phys. Rev. A*, vol. 84, p. 042320, Oct 2011.

[16] N. Friis, P. Köhler, E. Martín-Martínez, and R. A. Bertlmann, "Residual entanglement of accelerated fermions is not nonlocal," *Phys. Rev. A*, vol. 84, p. 062111, Dec 2011.

[17] N. Friis, A. R. Lee, D. E. Bruschi, and J. Louko, "Kinematic entanglement degradation of fermionic cavity modes," *Phys. Rev. D*, vol. 85, p. 025012, Jan 2012.

[18] M. Montero and E. Martín-Martínez, "Convergence of fermionic-field entanglement at infinite acceleration in relativistic quantum information," *Phys. Rev. A*, vol. 85, p. 024301, Feb 2012.

[19] N. Friis, A. R. Lee, and D. E. Bruschi, "Fermionic-mode entanglement in quantum information," *Phys. Rev. A*, vol. 87, p. 022338, Feb 2013.

[20] M.-C. Bañuls, J. I. Cirac, and M. M. Wolf, "Entanglement in fermionic systems," *Phys. Rev. A*, vol. 76, p. 022311, Aug 2007.

[21] P. Caban, K. Podlaski, J. Rembielinski, K. A. Smolinski, and Z. Walczak, "Entanglement and tensor product decomposition for two fermions," *Journal of Physics A: Mathematical and General*, vol. 38, no. 6, p. L79, 2005.

[22] N. Schuch, F. Verstraete, and J. I. Cirac, "Quantum entanglement theory in the presence of superselection rules," *Phys. Rev. A*, vol. 70, p. 042310, Oct 2004.

[23] F. Verstraete and J. I. Cirac, "Quantum nonlocality in the presence of superselection rules and data hiding protocols," *Phys. Rev. Lett.*, vol. 91, p. 010404, Jul 2003.

[24] S. D. Bartlett and H. M. Wiseman, "Entanglement constrained by superselection rules," *Phys. Rev. Lett.*, vol. 91, p. 097903, Aug 2003.

[25] N. Schuch, F. Verstraete, and J. I. Cirac, "Nonlocal resources in the presence of superselection rules," *Phys. Rev. Lett.*, vol. 92, p. 087904, Feb 2004.

[26] Q. Pan and J. Jing, "Degradation of nonmaximal entanglement of scalar and dirac fields in noninertial frames," *Phys. Rev. A*, vol. 77, p. 024302, Feb 2008.

[27] Q. Pan and J. Jing, "Hawking radiation, entanglement, and teleportation in the background of an asymptotically flat static black hole," *Phys. Rev. D*, vol. 78, p. 065015, Sep 2008.

[28] J. León and E. Martín-Martínez, "Spin and occupation number entanglement of dirac fields for noninertial observers," *Phys. Rev. A*, vol. 80, p. 012314, Jul 2009.

[29] S. Moradi, "Distillability of entanglement in accelerated frames," *Phys. Rev. A*, vol. 79, p. 064301, Jun 2009.

[30] D. C. M. Ostapchuk and R. B. Mann, "Generating entangled fermions by accelerated measurements on the vacuum," *Phys. Rev. A*, vol. 79, p. 042333, Apr 2009.

[31] J. Wang and J. Jing, "Quantum decoherence in noninertial frames," *Phys. Rev. A*, vol. 82, p. 032324, Sep 2010.

[32] S. Khan and M. K. Khan, "Relativistic quantum games in noninertial frames," *J. of Phys. A*, vol. 44, p. 355302, August 2011.

[33] A. Valentini, "Non-local correlations in quantum electrodynamics," *Phys. Lett. A*, vol. 153, no. 6, pp. 321 – 325, 1991.

[34] B. Reznik, "Entanglment from the vacuum," *Found. Phys.*, vol. 33, pp. 167–176, 2003.

[35] J. S. Benni Reznik, Alex Retzker, "Violating bell's inequalities in the vacuum," *Phys. Rev. A*, 2005.

[36] A. Pozas-Kerstjens and E. Martín-Martínez, "Harvesting correlations from the quantum vacuum," *Phys. Rev. D*, vol. 92, p. 064042, Sep 2015.

[37] S. Takagi, "On the response of a rindler particle detector. iii," *Prog. Theor. Phys.*, vol. 74, no. 3, pp. 501–510, 1985.

[38] S. Takagi, "Vacuum noise and stress induced by uniform acceleration: Hawking-unruh effect in rindler manifold of arbitrary dimension," *Prog. Theor. Phys. Supp.*, vol. 88, pp. 1–142, 1986.

[39] K. J. Hinton, "Particle detector equivalence," *Classical Quant. Grav.*, vol. 1, no. 1, p. 27, 1984.

[40] D. Hümmer, E. Martín-Martínez, and A. Kempf, "Renormalized unruh-dewitt particle detector models for boson and fermion fields," *Phys. Rev. D*, vol. 93, p. 024019, Jan 2016.

[41] E. Martín-Martínez, *Relativistic Quantum Information: developments in Quantum Information in general relativistic scenarios*. PhD thesis, Universidad Complutense de Madrid, 2011.

[42] S. DeWitt, *General Relativity: An Einstein Centenary Survey*. Cambridge University Press, 1979.

[43] M. Zych, I. Pikovski, F. Costa, and Č. Brukner, "General relativistic effects in quantum interference of "clocks"," *Journal of Physics: Conference Series*, vol. 723, no. 1, p. 012044, 2016.

[44] M. Zych, F. Costa, I. Pikovski, T. C. Ralph, and Č. Brukner, "General relativistic effects in quantum interference of photons," *Classical and Quantum Gravity*, vol. 29, no. 22, p. 224010, 2012.

[45] S. K. Joshi, J. Pienaar, T. C. Ralph, L. Cacciapuoti, W. McCutcheon, J. Rarity, D. Giggenbach, V. Makarov, I. Fuentes, T. Scheidl, E. Beckert, M. Bourennane, D. E. Bruschi, A. Cabello, J. Capmany, andJosé A. Carrasco, andAlberto Carrasco-Casado, andEleni Diamanti, andMiloslav Duusek, andDominique Elser, A. Gulinatti, R. H. Hadfield, T. Jennewein, R. Kaltenbaek, M. A. Krainak, H.-K. Lo, C. Marquardt, G. Milburn, M. Peev, A. Poppe, V. Pruneri, R. Renner, C. Salomon, J. Skaar, N. Solomos, M. Stipčević, J. P. Torres, M. Toyoshima, P. Villoresi, I. Walmsley, G. Weihs, H. Weinfurter, A. Zeilinger, M. Żukowski, and R. Ursina, *Space QUEST mission proposal: Experimentally testing decoherence due to gravity*. arXiv:1703.08036, 2017.

[46] O. Oreshkov, F. Costa, and Č. Brukner, "Quantum correlations with no causal order," *Nat Commun*, vol. 3, p. 1092, oct 2012.

[47] F. Costa and S. Shrapnel, "Quantum causal modelling," *New Journal of Physics*, vol. 18, no. 6, p. 063032, 2016.

[48] M. Hotta, "Quantum measurement information as a key to energy extraction from local vacuums," *Phys. Rev. D*, vol. 78, p. 045006, Aug 2008.

[49] M. Hotta, "Energy entanglement relation for quantum energy teleportation," *Phys. Lett. A*, vol. 374, no. 34, pp. 3416 – 3421, 2010.

[50] R. H. Jonsson, "Information travels in massless fields in 1+1 dimensions where energy cannot," *arXiv:1512.05065*, 2015.

[51] R. Schützhold and W. G. Unruh, "Quantum correlations across the black hole horizon," *Phys. Rev. D*, vol. 81, p. 124033, Jun 2010.

[52] W. G. Unruh, "Notes on black-hole evaporation," *Phys. Rev. D*, vol. 14, pp. 870–892, Aug 1976.

[53] A. Almheiri, D. Marolf, J. Polchinski, and J. Sully, "Black holes: complementarity or firewalls?," *J. High Energy Phys.*, vol. 2013, no. 2, pp. 1–20, 2013.

[54] S. L. Braunstein, S. Pirandola, and K. Życzkowski, "Better late than never: Information retrieval from black holes," *Phys. Rev. Lett.*, vol. 110, p. 101301, Mar 2013.

[55] B. R. Iyer and A. Kumar, "Detection of dirac quanta in rindler and black hole space-times and the xi quantisation scheme," *Journal of Physics A: Mathematical and General*, vol. 13, no. 2, p. 469, 1980.

[56] W. G. Unruh and R. M. Wald, "Evolution laws taking pure states to mixed states in quantum field theory," *Phys. Rev. D*, vol. 52, pp. 2176–2182, Aug 1995.

[57] E. Martín-Martínez, "Causality issues of particle detector models in qft and quantum optics," *Phys. Rev. D*, vol. 92, p. 104019, Nov 2015.

[58] A. Pozas-Kerstjens, J. Louko, and E. Martín-Martínez, *Degenerate detectors are unable to harvest spacelike entanglement.* To appear in Phys. Rev. D - arXiv:1703.02982, 2017.

[59] R. H. Jonsson, E. Martín-Martínez, and A. Kempf, "Information transmission without energy exchange," *Phys. Rev. Lett.*, vol. 114, p. 110505, Mar 2015.

[60] A. G. S. Landulfo, "Nonperturbative approach to relativistic quantum communication channels," *Phys. Rev. D*, vol. 93, p. 104019, May 2016.

[61] M. Paternostro, H. Jeong, and T. C. Ralph, "Violations of bell's inequality for gaussian states with homodyne detection and nonlinear interactions," *Phys. Rev. A*, vol. 79, p. 012101, Jan 2009.

[62] S. J. Summers and R. Werner, "The vacuum violates bell's inequalities," *Physics Letters A*, vol. 110, no. 5, pp. 257 – 259, 1985.

[63] S. J. Summers and R. Werner, "Bell's inequalities and quantum field theory. i. general setting," *Journal of Mathematical Physics*, vol. 28, no. 10, pp. 2440–2447, 1987.

[64] M. Hotta, "Quantum energy teleportation in spin chain systems," *J. Phys. Soc. Jpn.*, vol. 78, no. 3, p. 034001, 2009.

[65] L. Susskind, L. Thorlacius, and J. Uglum, "The stretched horizon and black hole complementarity," *Phys. Rev. D*, vol. 48, pp. 3743–3761, Oct 1993.

[66] G. Salton, R. B. Mann, and N. C. Menicucci, "Acceleration-assisted entanglement harvesting and rangefinding," *New J. Phys.*, vol. 17, no. 3, p. 035001, 2015.

[67] G. V. Steeg and N. C. Menicucci, "Entangling power of an expanding universe," *Phys. Rev. D*, vol. 79, p. 044027, Feb 2009.

[68] E. Martín-Martínez and N. C. Menicucci, "Cosmological quantum entanglement," *Classical Quant. Grav.*, vol. 29, no. 22, p. 224003, 2012.

[69] E. Martín-Martínez and N. C. Menicucci, "Entanglement in curved spacetimes and cosmology," *Classical Quant. Grav.*, vol. 31, no. 21, p. 214001, 2014.

[70] E. Martín-Martínez, A. R. H. Smith, and D. R. Terno, "Spacetime structure and vacuum entanglement," *Phys. Rev. D*, vol. 93, p. 044001, Feb 2016.

[71] E. Martín-Martínez, E. G. Brown, and a. A. K. William Donnelly, "Sustainable entanglement production from a quantum field," *Phys. Rev. A*, vol. 88, p. 052310, Nov 2013.

[72] E. G. Brown, W. Donnelly, A. Kempf, R. B. Mann, E. Martín-Martínez, and N. C. Menicucci, "Quantum seismology," *New J. Phys.*, vol. 16, no. 10, p. 105020, 2014.

[73] S. J. Olson and T. C. Ralph, "Extraction of timelike entanglement from the quantum vacuum," *Phys. Rev. A*, vol. 85, p. 012306, Jan 2012.

[74] S. J. Olson and T. C. Ralph, "Entanglement between the future and the past in the quantum vacuum," *Phys. Rev. Lett.*, vol. 106, p. 110404, Mar 2011.

[75] T. C. Ralph and N. Walk, "Quantum key distribution without sending a quantum signal," *New Journal of Physics*, vol. 17, no. 6, p. 063008, 2015.

[76] C. Sabín, B. Peropadre, M. del Rey, and E. Martín-Martínez, "Extracting past-future vacuum correlations using circuit qed," *Phys. Rev. Lett.*, vol. 109, p. 033602, Jul 2012.

[77] A. Pozas-Kerstjens and E. Martín-Martínez, "Entanglement harvesting from the electromagnetic vacuum with hydrogenlike atoms," *Phys. Rev. D*, vol. 94, p. 064074, Sep 2016.

[78] C. H. Bennett, D. P. DiVincenzo, J. A. Smolin, and W. K. Wootters, "Mixed-state entanglement and quantum error correction," *Phys. Rev. A*, vol. 54, pp. 3824–3851, Nov 1996.

[79] P. M. Hayden, M. Horodecki, and B. M. Terhal, "The asymptotic entanglement cost of preparing a quantum state," *Journal of Physics A: Mathematical and General*, vol. 34, no. 35, p. 6891, 2001.

[80] G. Vidal and R. F. Werner, "Computable measure of entanglement," *Phys. Rev. A*, vol. 65, p. 032314, Feb 2002.

[81] G. Vidal, "Entanglement monotones," *Journal of Modern Optics*, vol. 47, no. 2-3, pp. 355–376, 2000.

[82] M. A. Nielsen and I. L. Chuang, *Quantum Computation and Quantum Information*. Cambridge University Press, 2011.

[83] S. M. Barnett and S. J. D. Phoenix, "Entropy as a measure of quantum optical correlation," *Phys. Rev. A*, vol. 40, pp. 2404–2409, Sep 1989.

[84] K. K.-C. Ng, "Unruh-dewitt detector response along static and circular-geodesic trajectories for schwarzschild-ads black holes," Master's thesis, University of Waterloo, 2014.

[85] E. G. Brown, "Operational approaches to quantum correlations and particle creation in field theory," Master's thesis, Univeristy of Waterloo, 2015.

[86] R. Jonsson, *Decoupling of Information Propagation from Energy Propagation*. PhD thesis, University of Waterloo, 2016.

[87] D. R. Terno, "Localization of relativistic particles and uncertainty relations," *Phys. Rev. A*, vol. 89, p. 042111, Apr 2014.

[88] S. A. Fulling, "Nonuniqueness of canonical field quantization in riemannian spacetime," *Phys. Rev. D*, vol. 7, pp. 2850–2862, May 1973.

[89] P. C. W. Davies, "Scalar production in schwarzschild and rindler metrics," *J. Phys. A*, vol. 8, p. 609, 1975.

[90] P. G. Grove and A. C. Ottewill, "Notes on 'particle detectors'," *J of Phys. A*, vol. 16, no. 16, p. 3906, 1983.

[91] N. D. Brrell and P. C. W. Davies, *Quantum Fields in Curved Space*. Cambridge University Press, 1984.

[92] R. H. Jonsson, E. Martín-Martínez, and A. Kempf, "Quantum signaling in cavity qed," *Phys. Rev. A*, vol. 89, p. 022330, Feb 2014.

[93] J. Louko and A. Satz, "Transition rate of the unruh–dewitt detector in curved spacetime," *Classical Quant. Grav.*, vol. 25, no. 5, p. 055012, 2008.

[94] J. Louko and A. Satz, "How often does the unruh–dewitt detector click? regularization by a spatial profile," *Classical Quant. Grav.*, vol. 23, no. 22, p. 6321, 2006.

[95] A. Satz, "Then again, how often does the unruh–dewitt detector click if we switch it carefully?," *Classical Quant. Grav.*, vol. 24, no. 7, p. 1719, 2007.

[96] A. Blasco, L. J. Garay, M. Martín-Benito, and E. Martín-Martínez, "Violation of the strong huygen's principle and timelike signals from the early universe," *Phys. Rev. Lett.*, vol. 114, p. 141103, Apr 2015.

[97] E. Martín-Martínez and J. Louko, "(1 + 1)D calculation provides evidence that quantum entanglement survives a firewall," *Phys. Rev. Lett.*, vol. 115, p. 031301, Jul 2015.

[98] A. Blasco, L. J. Garay, M. Martín-Benito, and E. Martín-Martínez, "Timelike information broadcasting in cosmology," *Phys. Rev. D*, vol. 93, p. 024055, Jan 2016.

[99] M. O. Scully and M. S. Zubairy, *Quantum Optics*. Cambridge University Press, 1997.

[100] J. Louko and V. Toussaint, "Unruh-dewitt detector's response to fermions in flat spacetimes," *Phys. Rev. D*, vol. 94, p. 064027, Sep 2016.